Supplementary Information

Design Strategy and Molecular Level Understanding: Hole Transport Materials with Suitable Transition Dipole Orientation for OLEDs

Krishan Kumar, Sunil Kumar, Anirban Karmakar, Dipanshu Sharma, Feng-Rong Chen, Mangey Ram Nagar, Jwo-Huei Jou, Subrata Banik, Subrata Ghosh

Contents

1. General

General information on instrumentation and experimental work	
Instrument	Characterization
Jeol EXC NMR spectrometer	Both, proton (^{1}H) and carbon (^{13}C) NMR Spectra.
Bruker Maxix Impact HD instrument	Experimentally evaluated mass (HRMS) of the compounds. The theoretical mass of the compounds was calculated using isotope pattern software.
Shimadzu UV-2450 and Carry Eclips Fluorescence Spectrometer Agilent	The absorption and photoluminescence studies were carried out using 5 µM in DCM solution. Excitation wavelengths for **PhMeO, TolPz, PhPz, PhMePz,** and **TolMePz** were 327, 327, 329, 326, and 327 nm, respectively.
NETZSCH STA448 F1 JUPITOR	Thermogravimetric analysis (TGA) was performed at a heating rate of 10 °C/min under N_2 atmosphere.
Perkin Elmer DSC 8000 instruments	Differential scanning calorimetry (DSC) analysis was performed at a heating rate of 10 °C/min under N_2 atmosphere.
Metrohm Auto lab	Cyclic Voltammetry (CV) analysis
Agilent Technologies X-ray diffractometer	Single crystal diffraction studies

The starting substrates **MePz, MePzCHO,** and **HPzCHO** were synthesized following literature reported procedure.[1] The final compounds were synthesized following a modified literature procedure.[2]

2. Synthesis scheme and procedures:

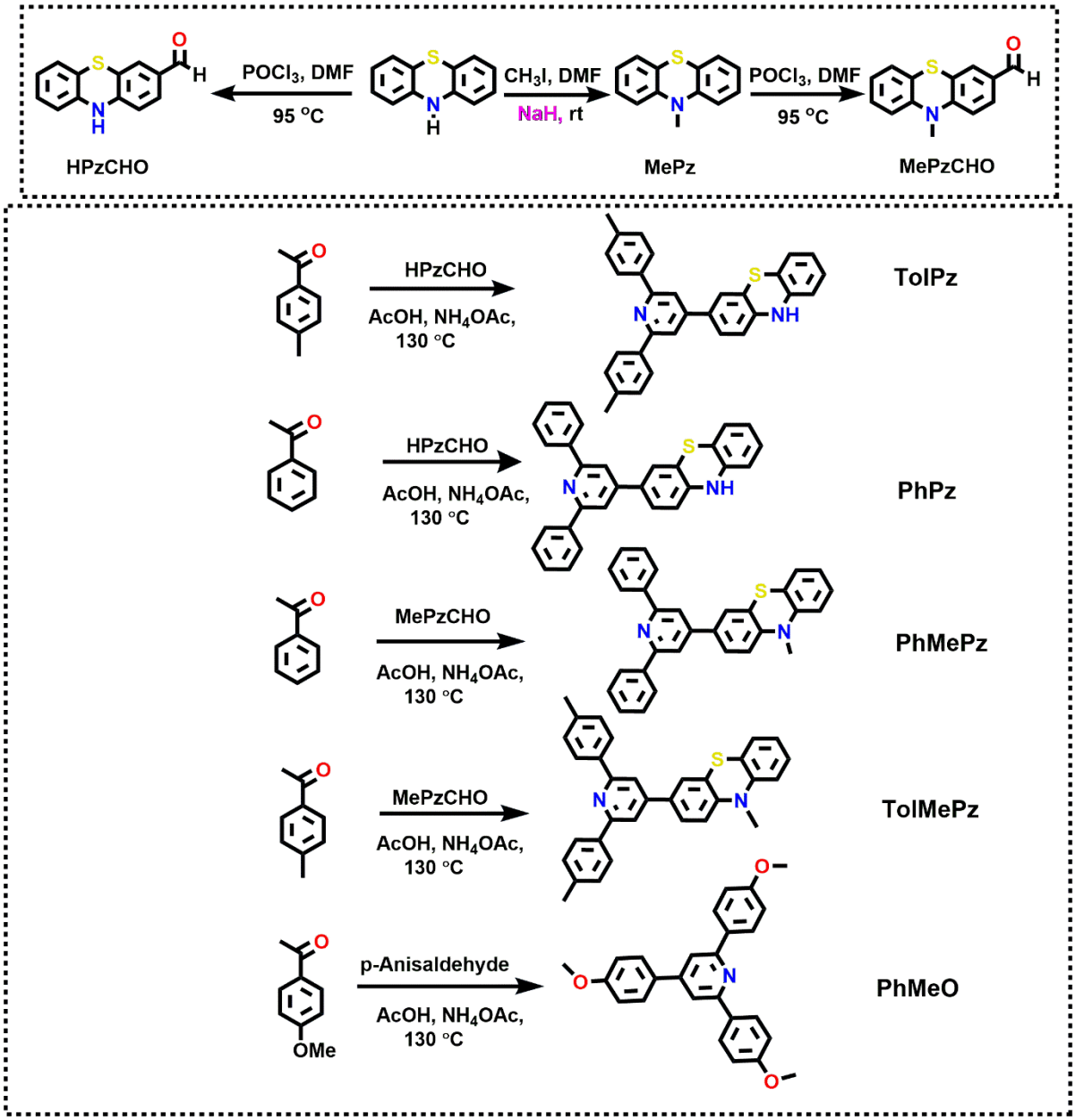

Scheme S1. Synthesis routes for **PhMeO**, **PhPz**, **PhMePz**, **TolPz** and **TolMePz**

Synthesis procedure for ***PhMeO***[3]:

A mixture of 4-methoxyacetophenone (3 eq), 4-methoxybenzaldehyde (1 eq), AcOH (15 ml), and ammonium acetate (8 eq) in 100 ml round-bottom flask was refluxed at 130 °C for 12h. After completion of the reaction, it was quenched with water and extracted with DCM. Finally, the DCM extract was washed with water followed by drying over sodium sulfate. The organic solvent was evaporated using rota-evaporator and the crude solid was purified by precipitation in methanol. Yield: 60%; ^{1}H NMR (500 MHz, $CDCl_3$): 8.13 (d, *J* = 8.90 Hz, 4H), 7.70 (s, 2H), 7.66 (d, *J* = 8.25 Hz, 2H), 7.01 (d, *J* = 8.25 Hz, 6H), 3.85 and 3.84 (s, 9H); ^{13}C NMR (125 MHz, $CDCl_3$): 160.34, 160.25, 156.78, 149.32, 132.37, 131.45, 128.27, 128.21, 115.10, 114.37, 113.92, 55.32, 55.29; HRMS (ESI); Calculated for $C_{26}H_{24}NO_3$ $[M+H]^+$: 398.1750, found: 398.1756.

Synthesis procedure for ***TolPz:***

A mixture of 4-methylacetophenone (3 eq), **HPzCHO** (1 eq), AcOH (15 ml), and ammonium acetate (8 eq) in 100 ml round-bottom flask was refluxed at 130 °C for 12h. After completion of the reaction, it was quenched with water and extracted with DCM. Finally, the DCM extract was washed with water followed by drying over sodium sulfate. Column chromatography was used to purify the crude product using 6% ethyl acetate-hexane mixture as the eluent; Yellow color solid; Yield: 40%; ^{1}H NMR (500 MHz, DMSO-*d6*): 8.89 (s, 1H), 8.21 (d, *J* = 6.85 Hz, 4H), 8.03 (s, 2H), 7.70-7.68 (m, 2H), 7.31 (d, *J* = 6.9 Hz, 4H), 7.02-6.94 (m, 2H), 6.85-6.72 (m, 3H), 2.36 (s, 6H); ^{13}C NMR (125 MHz, DMSO-*d6*): 156.20, 148.08, 142.88, 141.26, 138.53, 136.21, 130.92, 129.22, 127.64, 126.76, 126.61, 126.27, 124.86, 124.73, 122.11, 117.22, 116.16, 114.61, 114.57, 20.89; HRMS (ESI); Calculated for $C_{31}H_{23}N_2S$ $[M-H]^-$: 455.1576, found: 455.1570.

*Synthesis procedure for **PhPz**:*

A mixture of acetophenone (3 eq), **HPzCHO** (1 eq), AcOH (15 ml), and ammonium acetate (8 eq.) in 100 ml round-bottom flask was refluxed at 130 °C for 12h. After completion of the reaction, it was quenched with water and extracted with DCM. Finally, the DCM extract was washed with water followed by drying over sodium sulfate. Column chromatography was used to purify the crude product using 8% ethyl acetate-hexane mixture as the eluent; Yellow color solid; Yield: 45%; ^{1}H NMR (500 MHz, DMSO-*d6*): 8.89 (s, 1H), 8.32 (d, *J* = 6.85 Hz, 4H), 8.11 (s, 2H), 7.74-7.71 (m, 2H), 7.53-7.45 (m, 6H), 7.02-6.94 (m, 2H), 6.84-6.72 (m, 3H); ^{13}C NMR (125 MHz, DMSO-*d6*): 156.87, 148.81, 143.49, 141.73, 139.46, 131.27, 129.65, 129.18, 128.20, 127.47, 127.23, 126.83, 125.46, 122.69, 117.77, 116.67, 155.82, 115.16, 115.11; HRMS (ESI): Calculated for $C_{29}H_{21}N_2S$ $[M+H]^+$: 429.1419, found: 429.1414.

*Synthesis procedure for **PhMePz**:*[4]

A mixture of acetophenone (3 eq), **MePzCHO** (1 eq), AcOH (15 ml), and ammonium acetate (8 eq) in 100 ml round-bottom flask was refluxed at 130 °C for 12h. After completion of the reaction, it was quenched with water and extracted with DCM. Finally, the DCM extract was washed with water followed by drying over sodium sulfate. Column chromatography was used to purify the crude product using 5% ethyl acetate-hexane mixture as the eluent; Yellow color solid; Yield: 40%; ^{1}H NMR (500 MHz, $CDCl_3$): 8.16-8.15 (m, 4H), 7.75 (s, 2H), 7.49-7.39 (m, 8H), 7.19-7.12 (m, 2H), 6.93-6.90 (m, 1H), 6.79-6.75 (m, 2H), 3.29 (s, 3H); ^{13}C NMR (125 MHz, $CDCl_3$): 157.32, 148.57, 146.41, 145.06, 139.47, 132.71, 128.93, 128.60, 127.56, 127.14, 127.03, 126.11, 125.34, 124.07, 122.74, 122.59, 116.08, 114.23, 114.18, 35.26; HRMS (ESI): Calculated for $C_{30}H_{23}N_2S$ $[M+H]^+$: 443.1576, found: 443.1579.

*Synthesis procedure for **TolMePz**:*

A mixture of 4-methylacetophenone (3 eq), **MePzCHO** (1 eq) AcOH (15 ml) and ammonium acetate (8 eq.) in 100 ml round-bottom flask was refluxed at 130 °C for 12h. After completion

of the reaction, it was quenched with water and extracted with DCM. Finally, the DCM extract was washed with water followed by drying over sodium sulfate. Column chromatography was used to purify the crude product using 3% ethyl acetate-hexane mixture as the eluent; Yellow color solid; Yield: 45%; ^{1}H NMR (500 MHz, $CDCl_3$): 7.98 (d, *J* = 6.85 Hz, 4H), 7.65 (s, 2H), 7.40 (s, 2H), 7.20 (d, *J* = 7.55 Hz, 4H), 7.08-7.06 (m, 2H), 6.87-6.84 (m, 1H), 6.77-6.71 (m, 2H), 3.27 (s, 3H), 2.32 (s, 6H); ^{13}C NMR (125 MHz, $CDCl_3$): 157.30, 148.49, 146.40, 145.18, 138.86, 136.83, 133.08, 129.33, 127.59, 127.20, 126.93, 126.17, 125.44, 124.10, 122.76, 122.70, 115.58, 114.27, 114.20, 35.35, 21.29; HRMS (ESI): Calculated for $C_{32}H_{27}N_2S$ $[M+H]^+$: 471.1889, found: 471.1889.

3. Copies of ^{1}H and ^{13}C NMR spectra

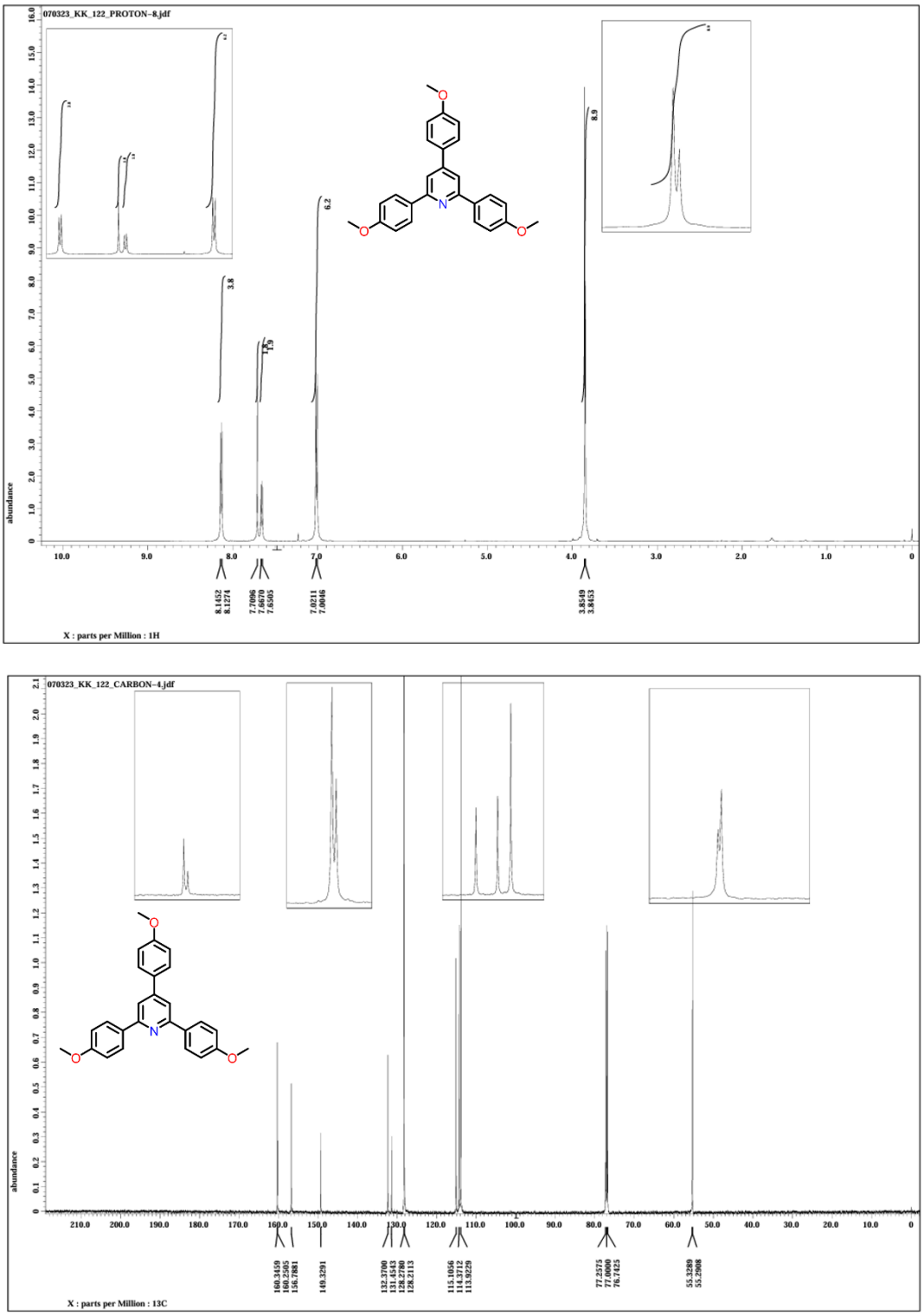

Fig. S1. ^{1}H and ^{13}C NMR spectra of **PhMeO**

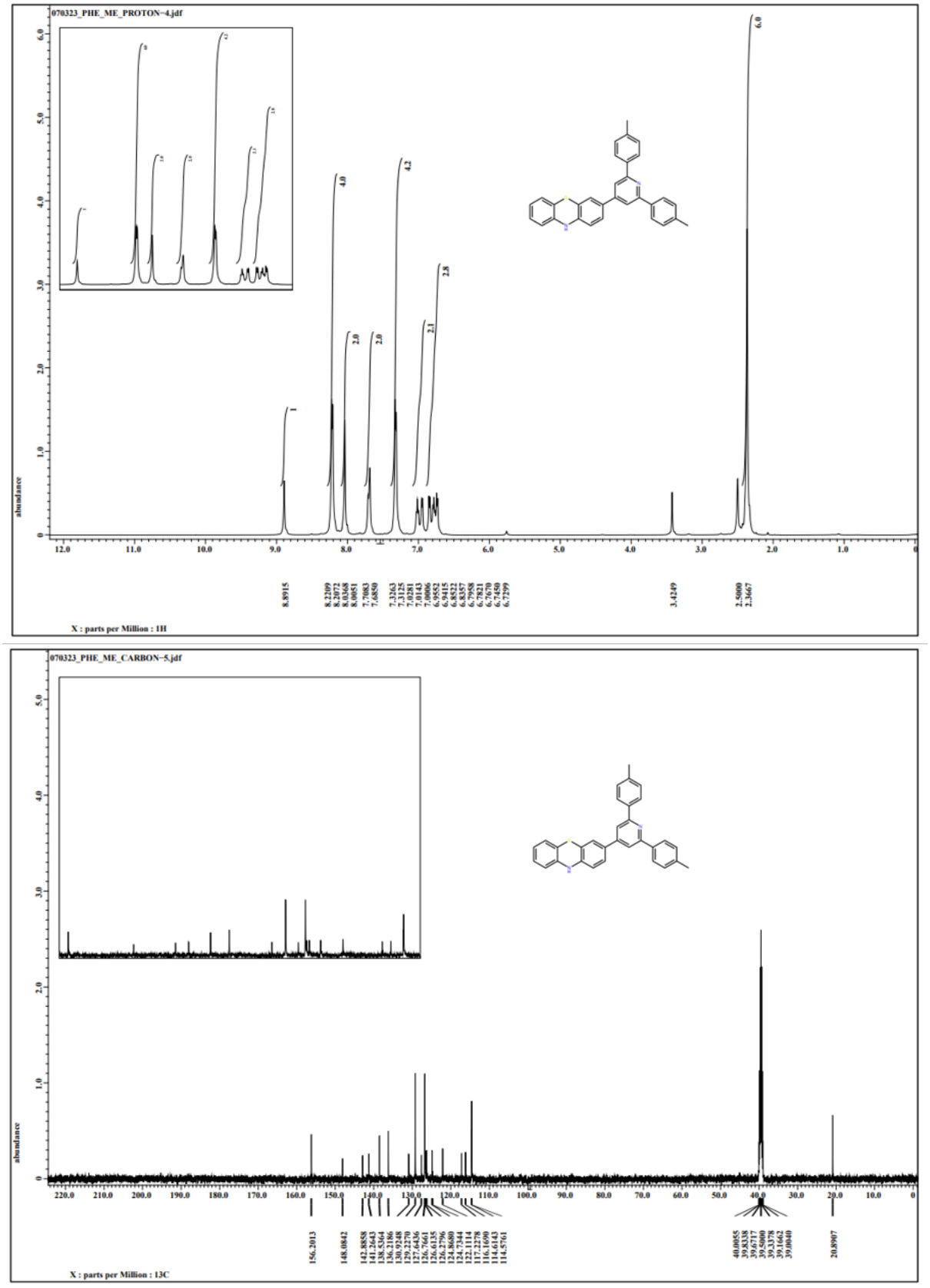

Fig. S2. ^{1}H and ^{13}C NMR spectra of **TolPz**

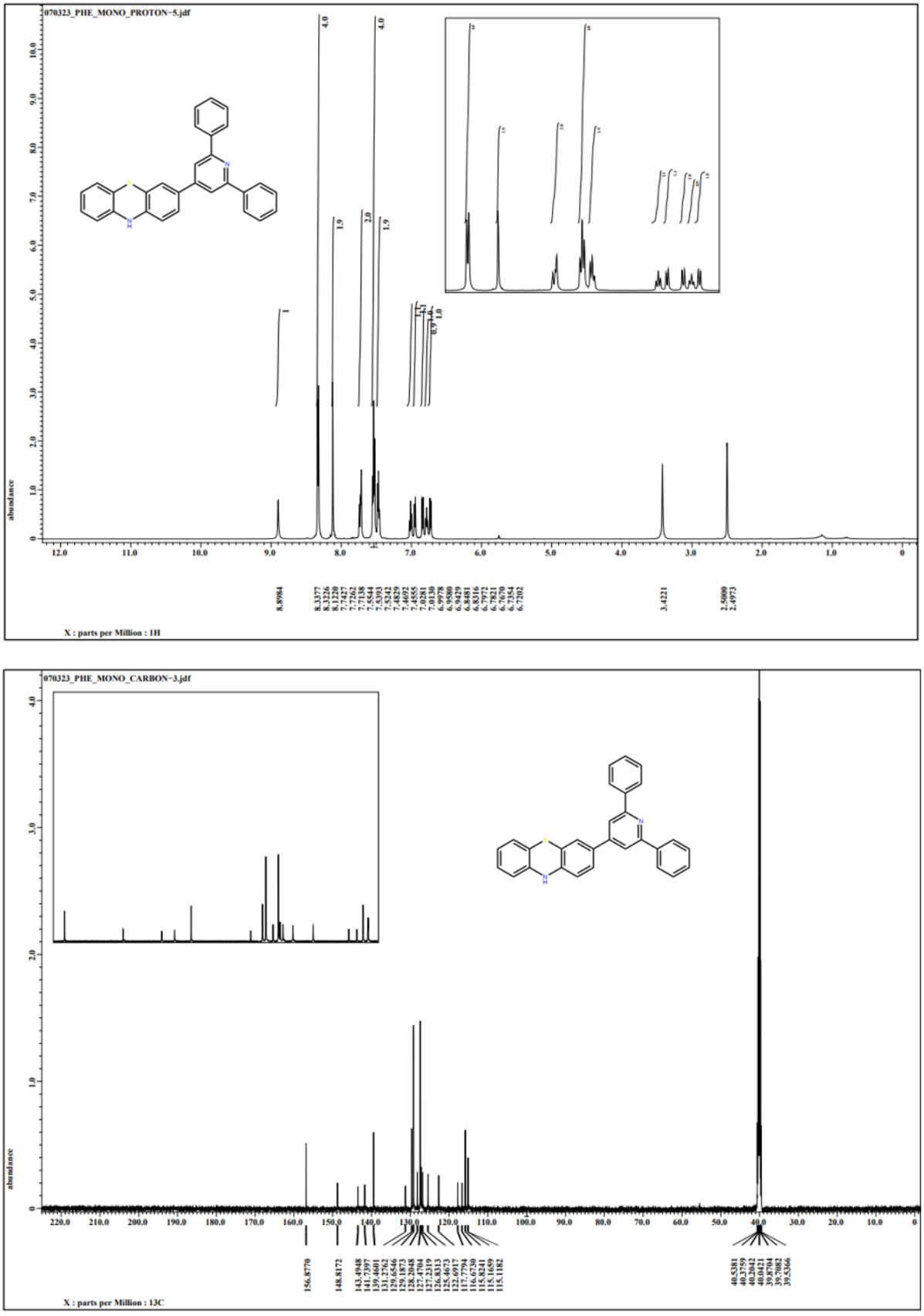

Fig. S3. ^{1}H and ^{13}C NMR spectra of **PhPz**

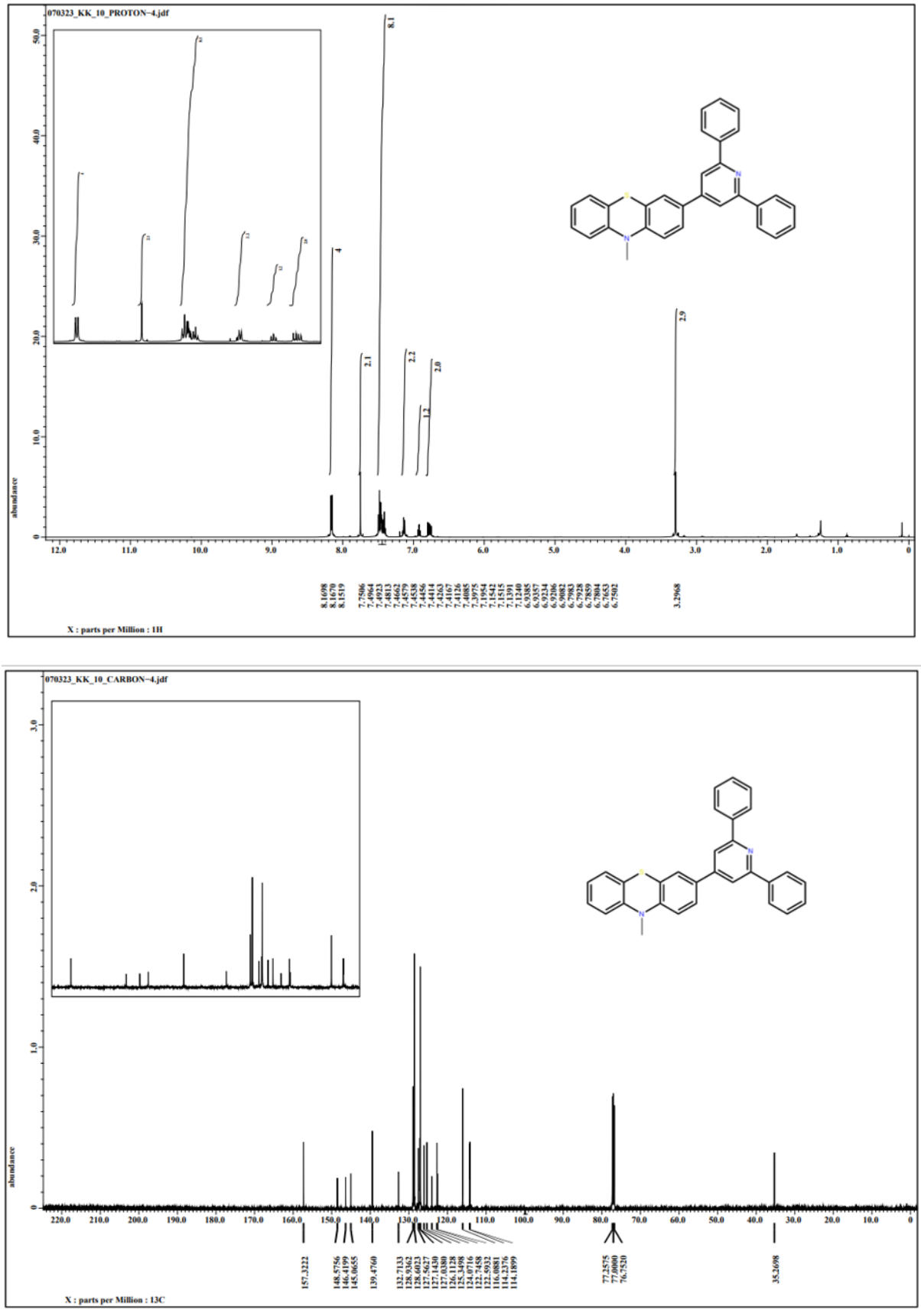

Fig. S4. ^{1}H and ^{13}C NMR spectra of **PhMePz**

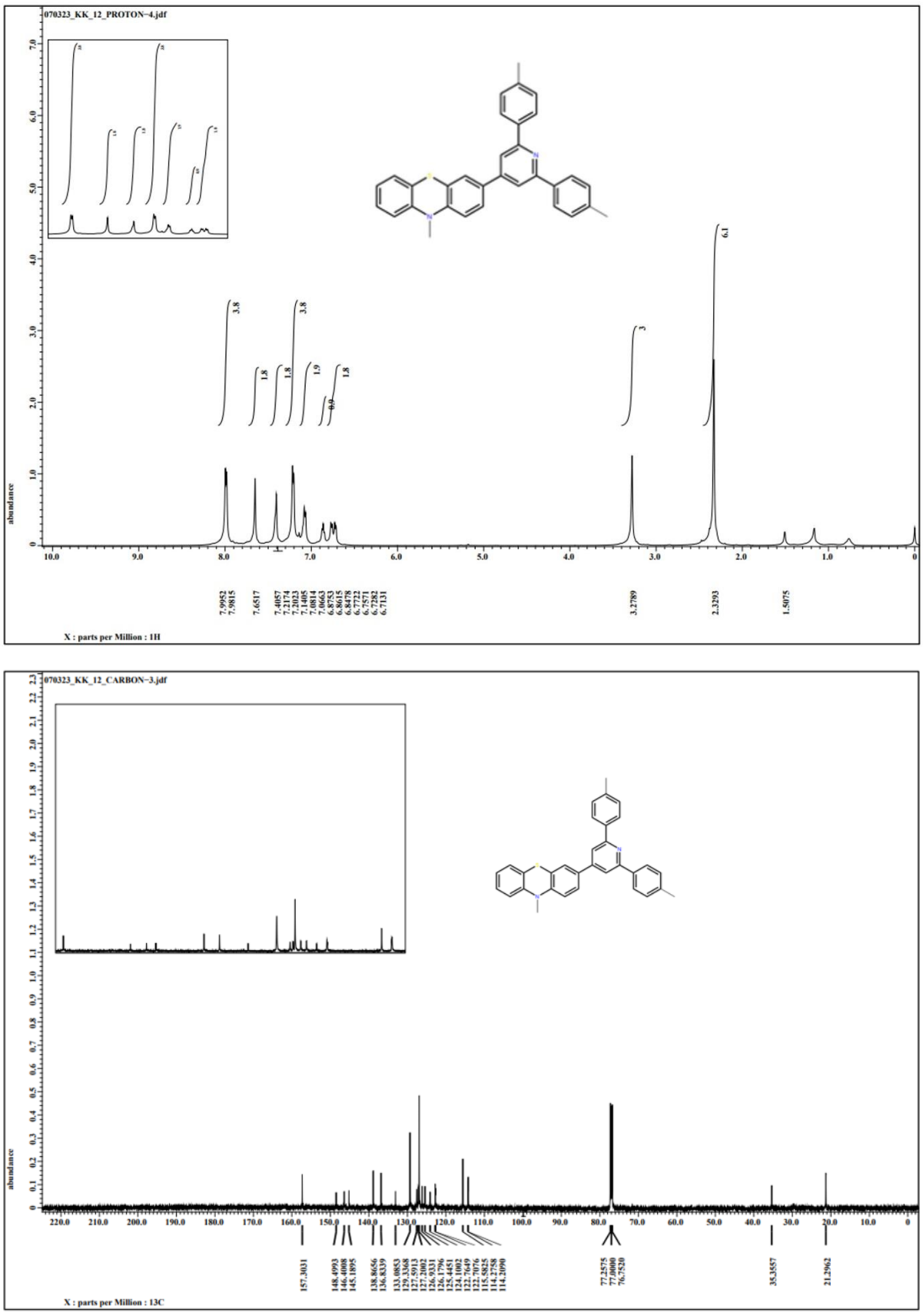

Fig. S5. ^{1}H and ^{13}C NMR spectra of **TolMePz**

4. HRMS

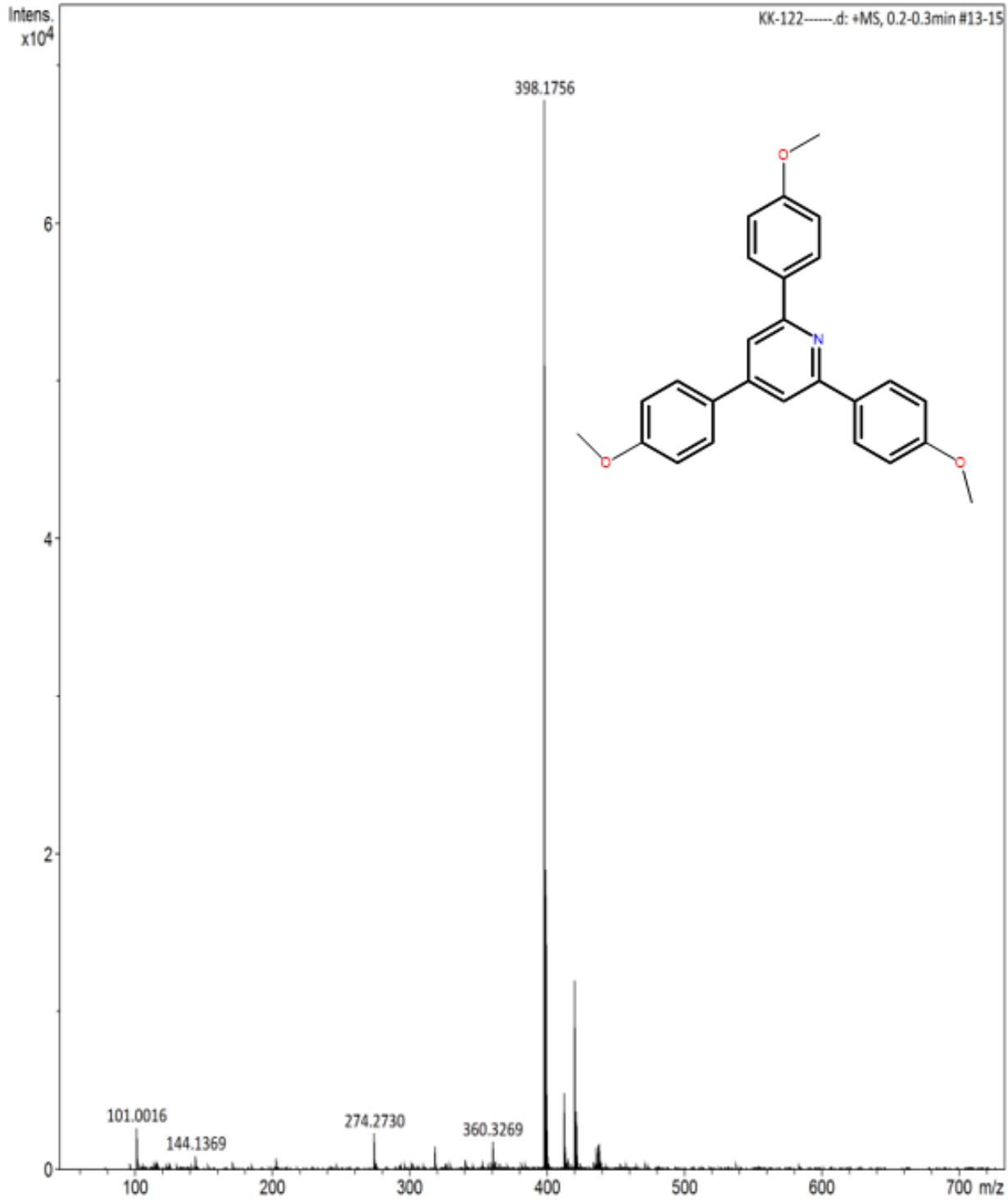

Fig. S6. HRMS spectra of **PhMeO**

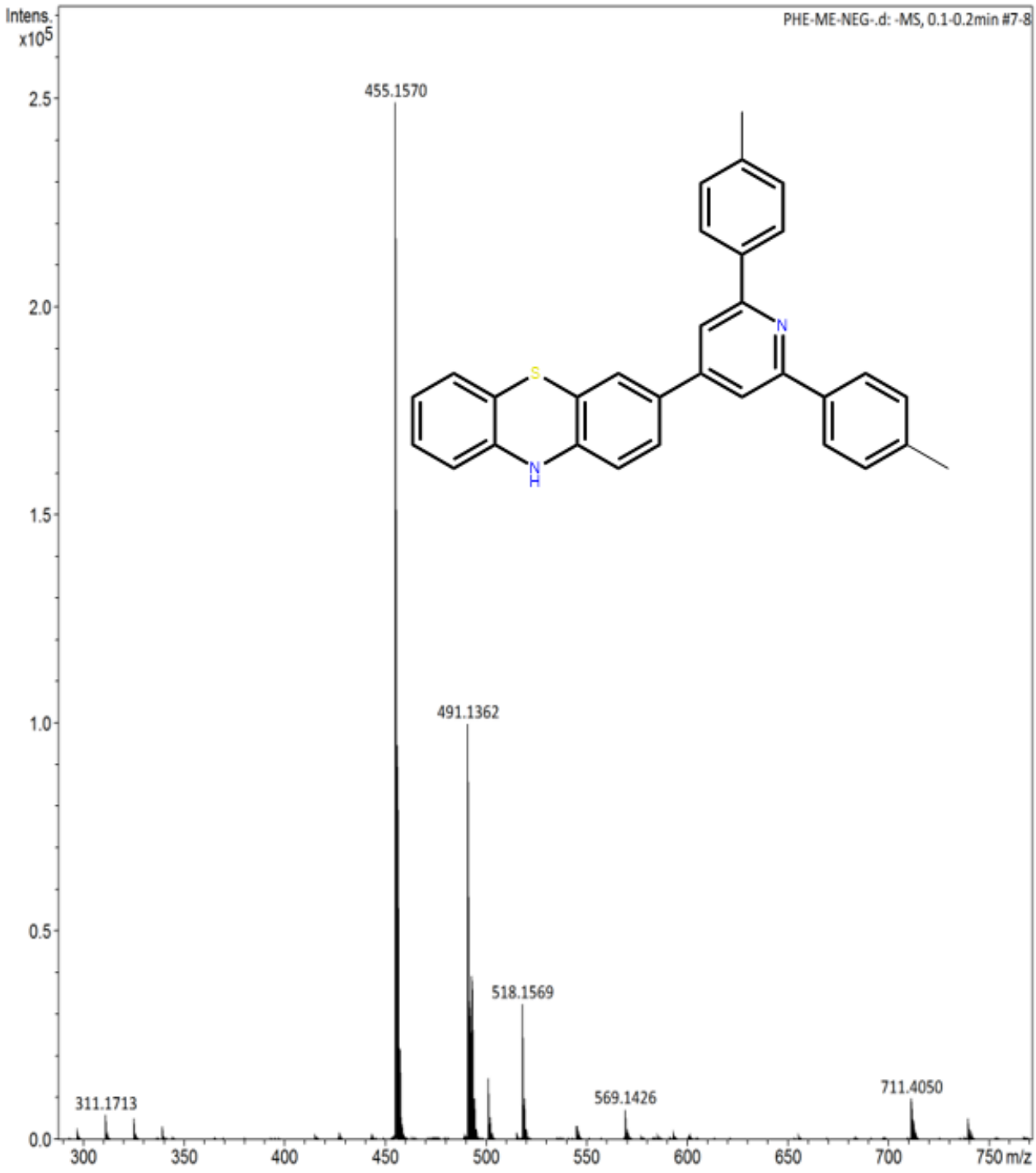

Fig. S7. HRMS spectra of **TolPz**

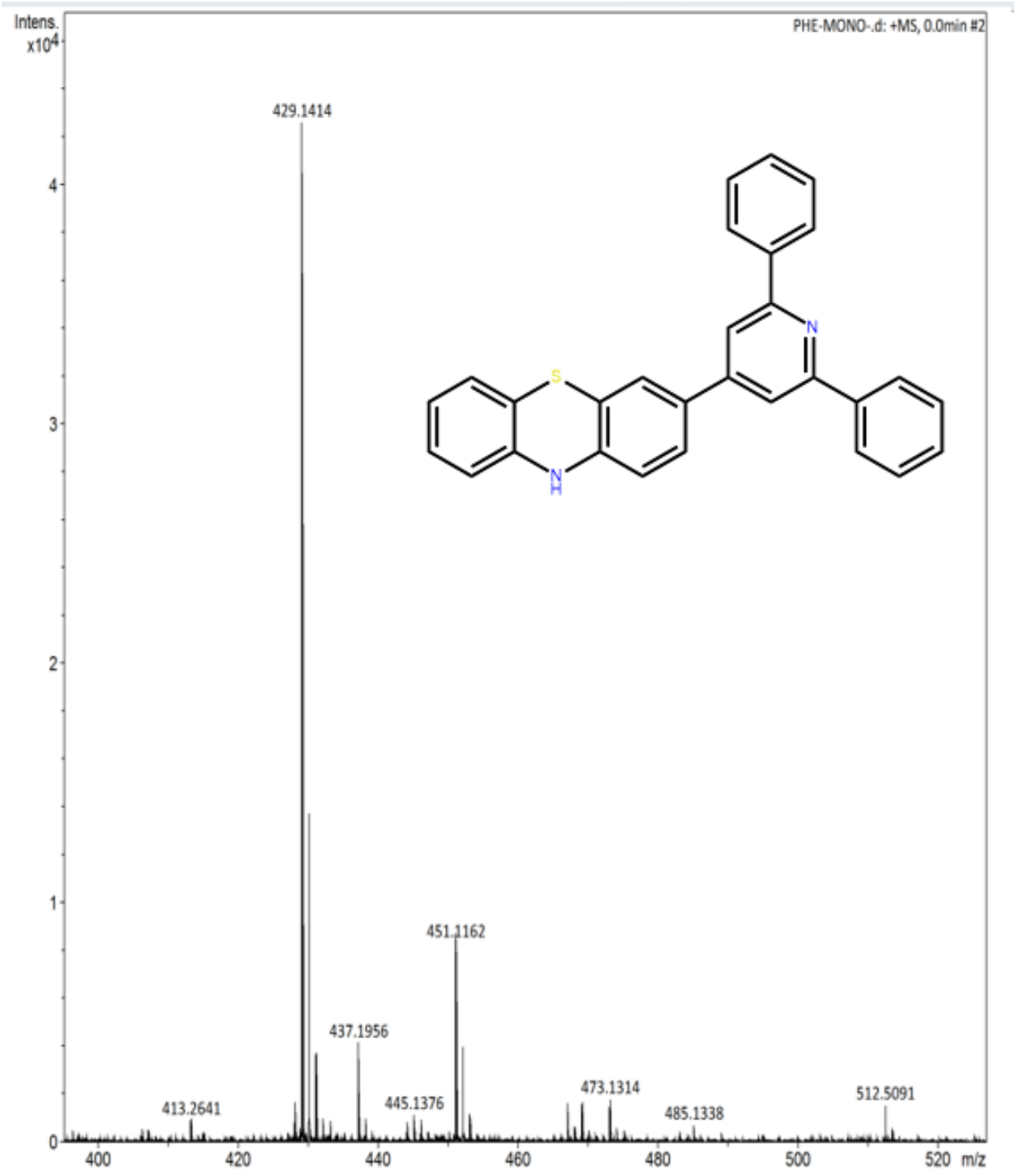

Fig. S8. HRMS spectra of **PhPz**

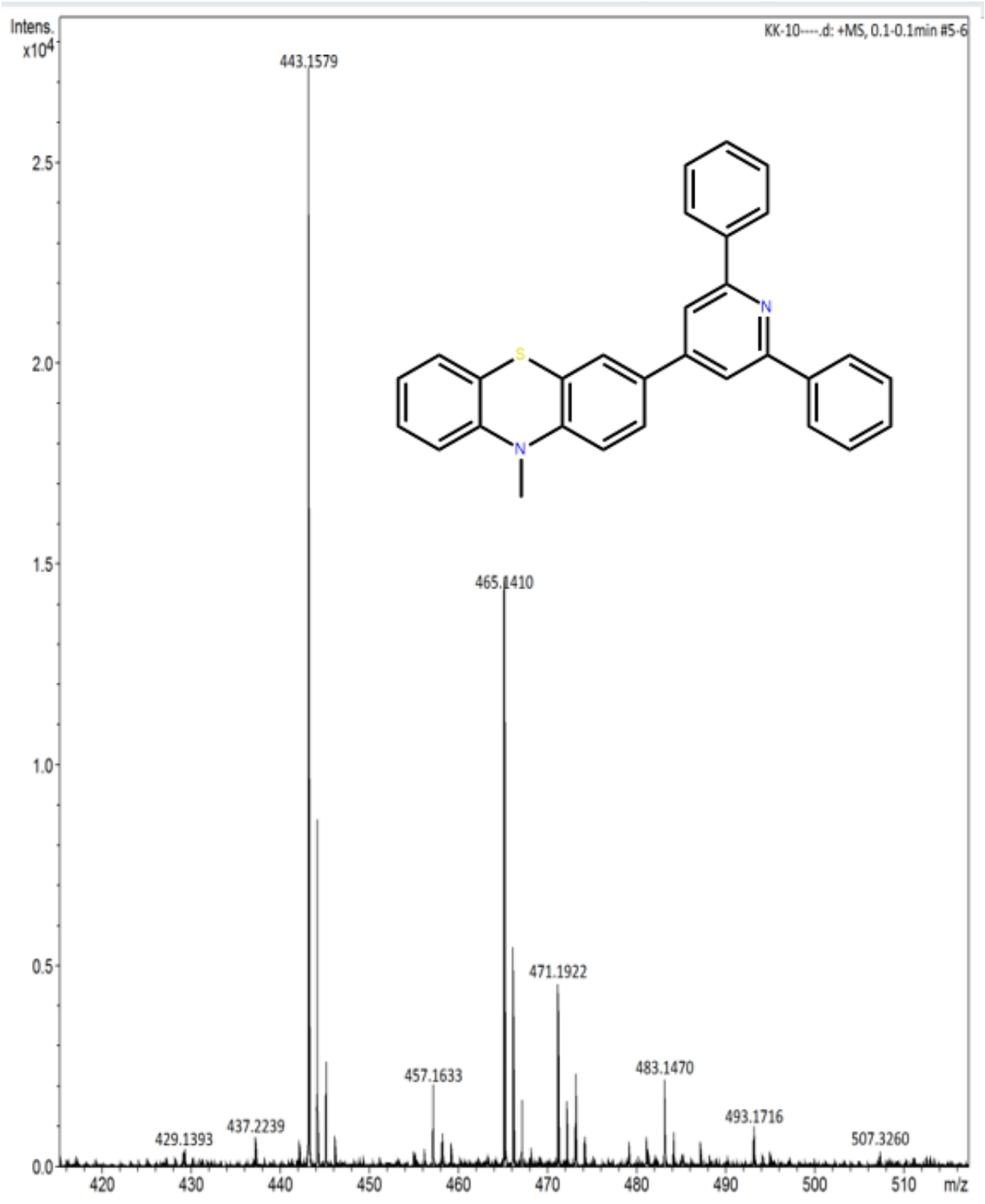

Fig. S9. HRMS spectra of **PhMePz**

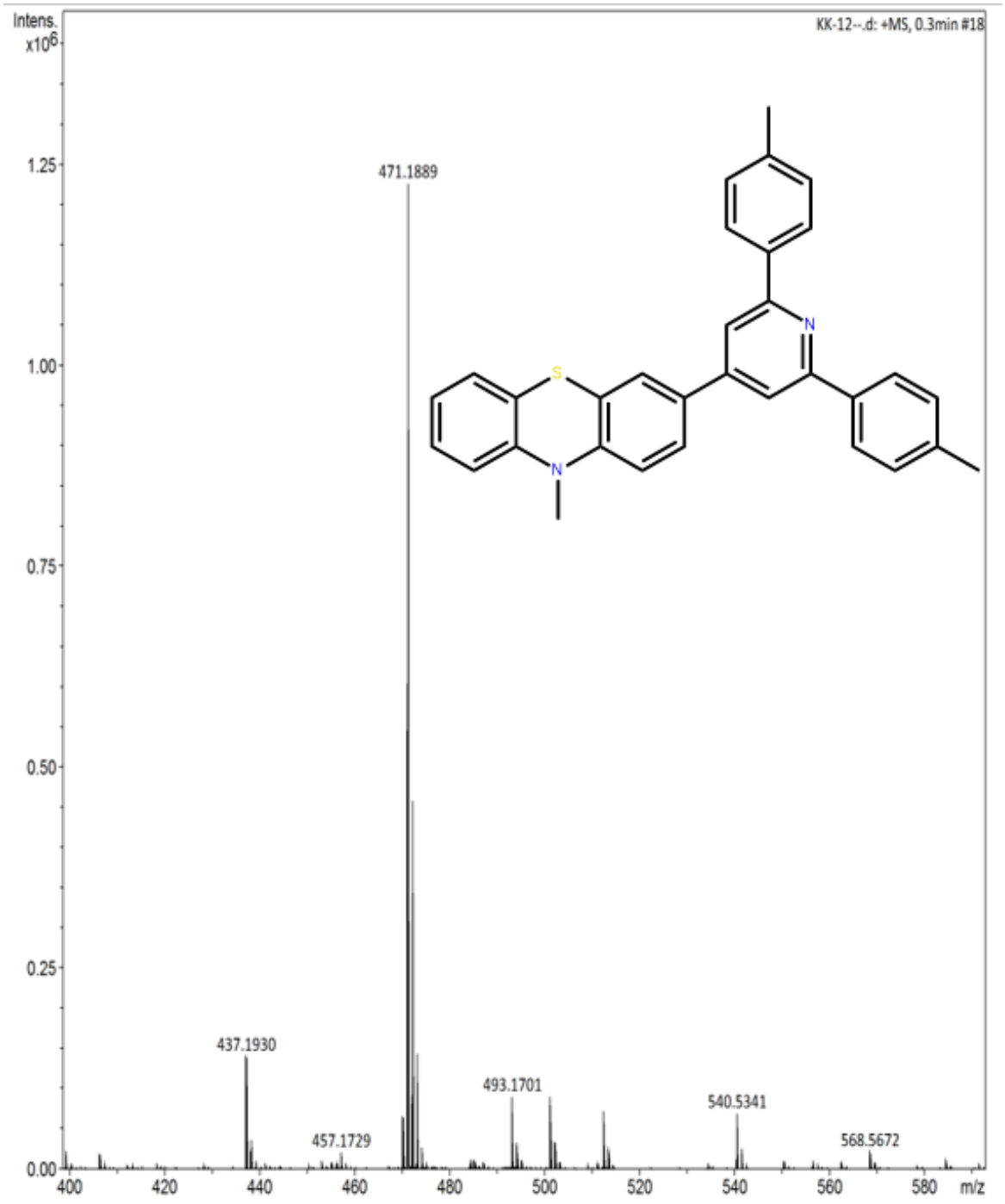

Fig. S10. HRMS spectra of **TolMePz**

5.Theoretical and experimental results

Table S1: Computed HOMO and LUMO energies (in eV) with three different density functionals.

Molecule	HOMO				LUMO			
	Exp.	B3LYP	PBE0	CAM-B3LYP	Exp.	B3LYP	PBE0	CAM-B3LYP
PhMePz	-5.12	-5.45	-5.68	-6.79	-1.50	-1.70	-1.59	-0.48
PhMeO	-5.34	-5.84	-6.06	-7.16	-1.68	-1.49	-1.38	-0.28
PhPz	-5.00	-5.42	-5.64	-6.76	-1.36	-1.69	-1.59	-0.48
TolMePz	-5.13	-5.45	-5.67	-6.79	-1.51	-1.65	-1.53	-0.43
TolPz	-5.00	-5.41	-5.63	-6.75	-1.37	-1.64	-1.54	-0.43
RMSD		0.37	0.60	1.69		0.27	0.27	1.19

Table S2: Computed λ_{max}(in nm) with three different density functionals.

Molecule	Exp.	B3LYP	PBE0	CAM-B3LYP
PhMeO	280	297.72	288.17	260.19
PhMePh	270	285.79	274.01	252.24
PhPz	271	284.62	272.9	253.69
TolMePz	269	285.31	274.72	252.73
TolPz	269	284.3	274.28	253.69
RMSD		14.9	5.4	20.0

Table S3: Comparison between gas-phase and solvent corrected HOMO/LUMO energies against experimental values. The optimization in each phase were carried out using B3LYP/6-311G(d,p) model.

	HOMO (eV)			**LUMO (eV)**		
	Gas-phase	DCM solvent	Experimental	Gas-phase	DCM solvent	Experimental
PhMeO	-5.41	-5.45	-5.12	-1.55	-1.70	-1.50
PhMePh	-5.37	-5.45	-5.13	-1.46	-1.65	-1.51
PhPz	-5.61	-5.84	-5.34	-1.26	-1.49	-1.68
TolMePz	-5.35	-5.41	-5.00	-1.47	-1.64	-1.37
TolPz	-5.38	-5.42	-5.00	-1.55	-1.69	-1.36

6.TD-DFT analysis

6.1. Transition energies, oscillator strengths and MO involved of some intense transitions:

Table S4. TD-DFT analysis for electronic transitions of **PhMePz**. Transitions with oscillator strengths (f) and MOs with coefficients greater than 0.15 and 0.20, respectively, are reported. Here, H and L stand for HOMO and LUMO, respectively.

S.No.	Transition Energy (eV)/Wavelength (nm)	Nature of transitions MOs involved Coefficients	f
1.	3.2585/ 380.50	H→L 0.68770	0.3190
2.	4.0637/ 305.10	H-1→L 0.66574	0.2975
3.	4.3383 / 285.79	H-2→L 0.46907 H→L+4 0.40603	0.9661
5.	4.9059 / 252.73	H-5→L 0.25111 H-3→L+1 0.56175	0.5176
6.	4.9385 / 251.06	H-4→L 0.41683 H-3→L 0.30761 H→L+8 0.27256	0.2461

Table S5. TD-DFT analysis for electronic transitions of **TolMePz.** Transitions with oscillator strengths (f) and MOs with coefficients greater than 0.24 and 0.20, respectively, are reported. Here, H and L stand for HOMO and LUMO, respectively.

S.No.	Transition Energy (eV)/Wavelength (nm)	Nature of transitions MOs involved Coefficients	f
1.	3.2913 / 376.70	H→L 0.68594	0.3299
2.	3.9517 / 313.75	H-1→L 0.65970	0.3411
3.	4.3457 / 285.31	H-2→L 0.41403 H→L+4 0.35836	1.1506
4.	4.6191 / 268.41	H-3→L+1 0.62013	0.2453
5.	4.6937 / 264.15	H-3→L+1 0.57764	0.4499

Table S6. TD-DFT analysis for electronic transitions of **PhMeO.** Transitions with oscillator strengths (f) and MOs with coefficients greater than 0.21 and 0.20, respectively, are reported. Here, H and L stand for HOMO and LUMO, respectively.

S.No.	Transition Energy (eV)/Wavelength (nm)	Nature of transitions MOs involved Coefficients	f
1.	3.7573 / 329.98	H→L 0.68064	0.3097
2.	4.1645 / 297.72	H-2→L 0.28713 H-1→L 0.41813 H→L+1 0.47997	1.2231
3.	4.3151 / 287.33	H-1→L+1 0.66452	0.5455
4.	4.4433 / 279.04	H-2→L+1 0.68590	0.2113
5.	5.0604 / 245.01	H→L+5 0.66441	0.2553
6.	5.4141 / 229.00	H-1 →L+5 0.65587	0.3034

Table S7. TD-DFT analysis for electronic transitions of **TolPz.** Transitions with oscillator strengths (f) and MOs with coefficients greater than 0.24 and 0.20, respectively, are reported. Here, H and L stand for HOMO and LUMO, respectively.

S.No.	Transition Energy (eV)/Wavelength (nm)	Nature of transitions MOs involved Coefficients	f
1.	3.2689 / 379.29	H→L 0.68527	0.3935
2.	3.9554 / 313.46	H-1→L 0.66941	0.3422
3.	4.0857 / 303.46	H→L+3 0.65855	0.3422
4.	4.3610 / 284.30	H-2→L 0.45707 H-1→L 0.41607	1.2112
5.	4.6455 / 266.89	H-3→L+1 0.27729 H -2→L+1 0.59247	0.3183
6.	4.6977 / 263.92	H-1→L+1 0.50033	0.2773

Table S8. TD-DFT analysis for electronic transitions of **PhPz.** Transitions with oscillator strengths (f) and MOs with coefficients greater than 0.11 and 0.20, respectively, are reported. Here, H and L stand for HOMO and LUMO, respectively.

S.No.	Transition Energy (eV)/Wavelength (nm)	Nature of transitions MOs involved Coefficients	f
1.	3.2383 / 382.87	H→L 0.68728	0.3829
2.	4.0823 / 303.71	H→L+3 0.56303	0.2529
3.	4.3561 / 284.62	H-2→L 0.54626	1.0230
4.	4.9133 / 252.35	H-4→L 0.25215 H-3→L+1 0.57304	0.5093
5.	5.0291 / 246.53	H-5→L 0.25830	0.1627
6.	5.0417 / 245.92	H-2→L+2 0.53671	0.1755

6.2. **Calculated UV-visible spectrum**

The plots were obtained using GaussView software, where the molar absorptivity of the electronic transitions (in $Lmol^{-1}cm^{-1)}$ is plotted with a Gaussian band shape to match the conventional UV-vis spectrum of experiments. The left-axis of the spectra presented below is the molar absorptivity, and the right-axes are the oscillator strength. The relation between the oscillator strength (*f*) value and molar absorptivity with a Gaussian fitting is given by[5]

$$\varepsilon_i(\tilde{\upsilon}) = \frac{\sqrt{\pi}e^2N}{1000\ln(10)c^2m_e}\frac{f_i}{\sigma}exp\left[-(\frac{\tilde{\upsilon}-\tilde{\upsilon}_i}{\sigma})^2\right]$$

Here, N, c, e, m_e, are Avogadro's number, speed of light, charge of an electron and mass of an electron, respectively. $\tilde{\upsilon}$ and $\tilde{\upsilon}_i$are the energy of incident radiation and excitation energy in wavenumbers, respectively. σ is the standard deviation in wavenumber unit. As default, the GaussView uses σ value equal to 0.4 eV.

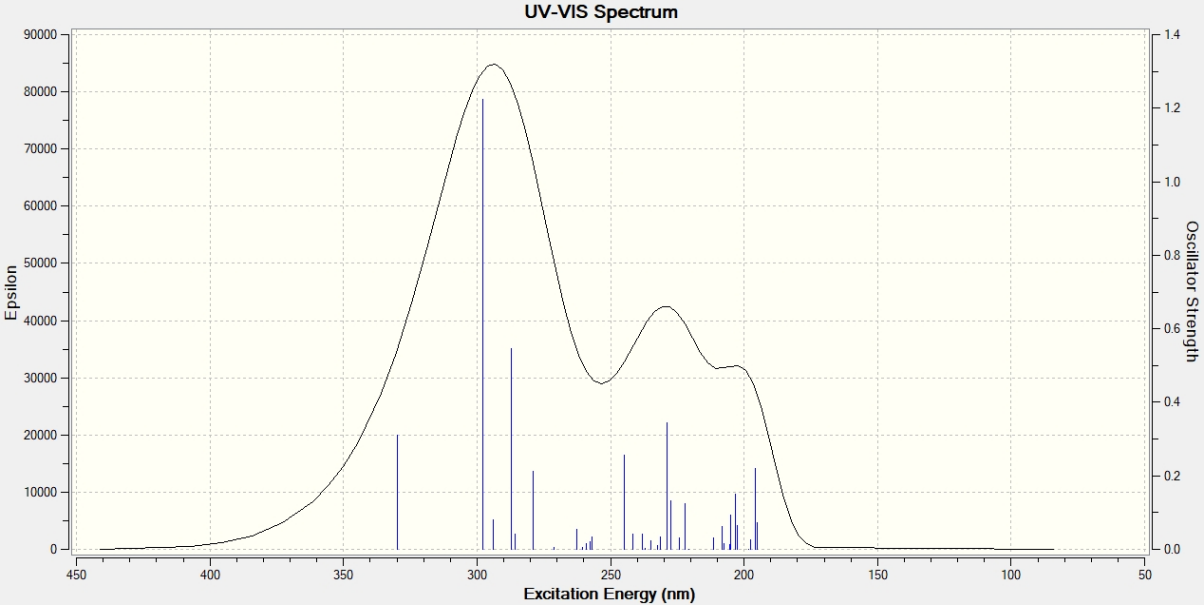

Fig. S11. Computed UV-vis spectrum of **PhMeO** with TD-DFT. The left-axis is the molar absorptivity fitted with a Gaussian band width of HWFM value 0.4 eV

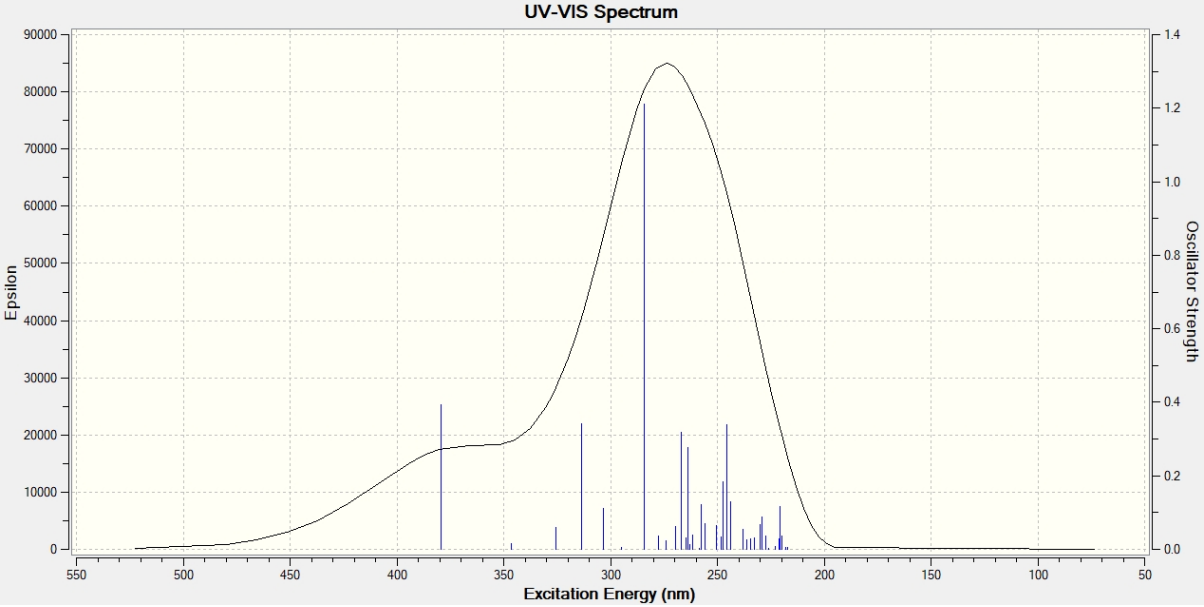

Fig. S12. Computed UV-vis spectrum of **TolPz** with TD-DFT. The left-axis is the molar absorptivity fitted with a Gaussian band width of HWFM value 0.4 eV.

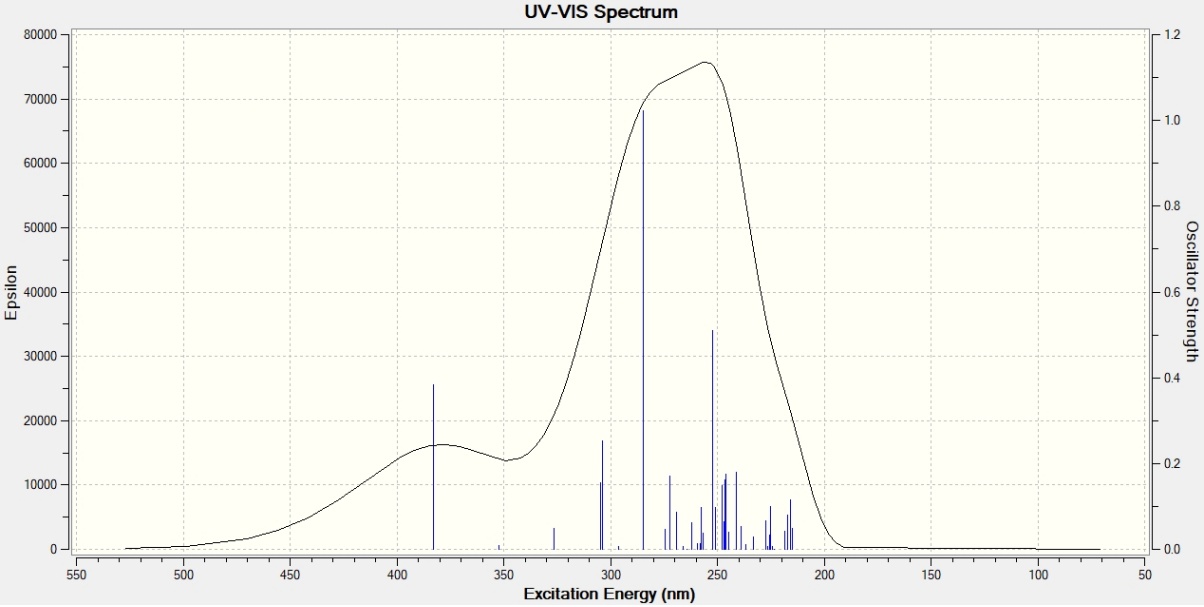

Fig. S13. Computed UV-vis spectrum of **PhPz** with TD-DFT. The left-axis is the molar absorptivity fitted with a Gaussian band width of HWFM value 0.4 eV.

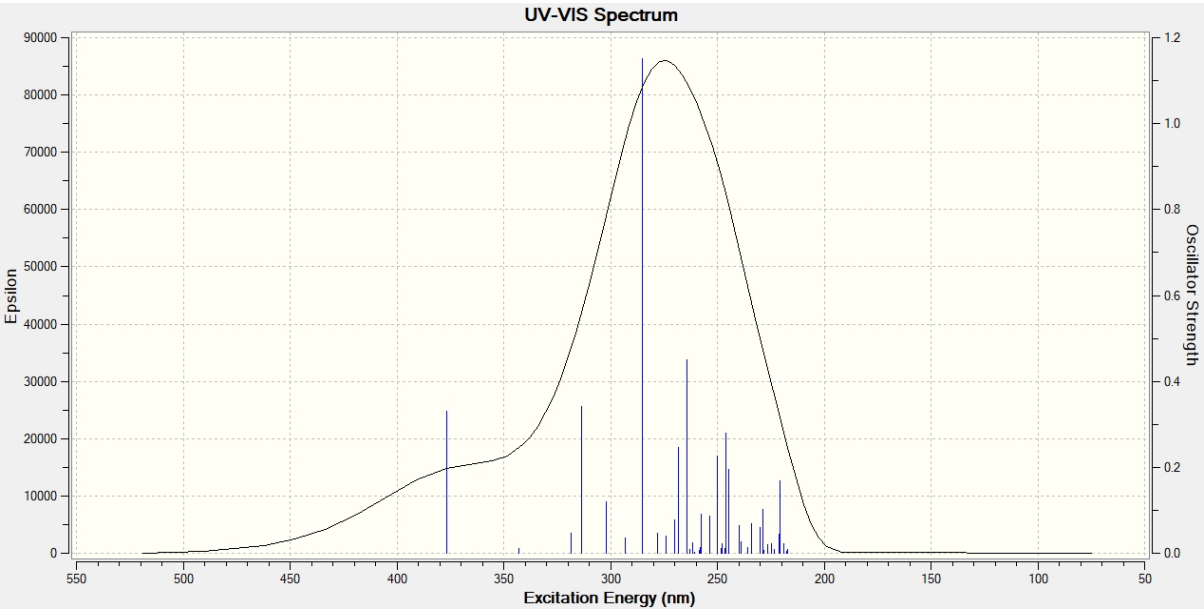

Fig. S14. Computed UV-vis spectrum of **TolMePz** with TD-DFT. The left-axis is the molar absorptivity fitted with a Gaussian band width of HWFM value 0.4 eV.

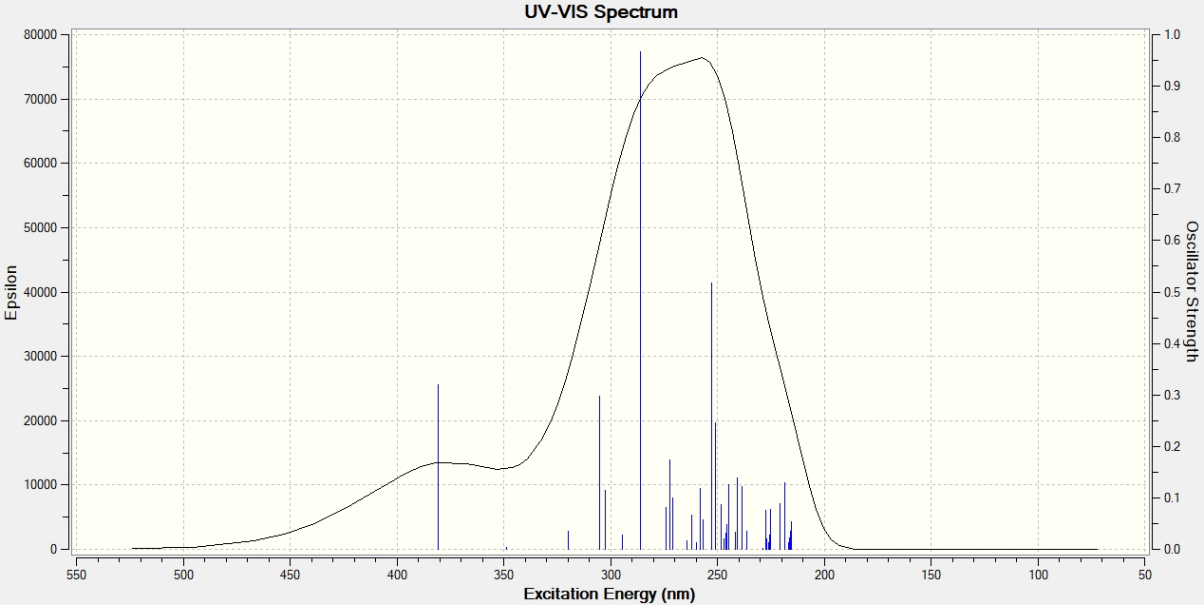

Fig. S15. Computed UV-vis spectrum of **PhMePz** with TD-DFT. The left-axis is the molar absorptivity fitted with a Gaussian band width of HWFM value 0.4 eV.

Table S9: Charge transfer distances and magnitude of charge transfer for each molecule: computed with CAM-B3LYP method and 6-311G(d,p) basis set.

Molecule	S_1		S_2		T_1		T_2	
	D_{CT} (Å)	Q_{CT}	D_{CT} (Å)	Q_{CT}	D_{CT} (Å)	Q_{CT}	D_{CT} (Å)	Q_{CT}
PhMeO	1.64	0.55	0.30	0.46	0.50	0.33	1.04	0.44
PhMePh	2.27	0.68	2.39	0.62	1.83	0.45	0.11	0.32
PhPz	2.01	0.64	2.55	0.62	1.62	0.46	0.33	0.31
TolMePz	2.16	0.68	2.16	0.58	1.69	0.42	0.11	0.34
TolPz	1.88	0.64	2.52	0.62	1.53	0.45	0.34	0.32

7. Cartesian coordinates

Cartesian coordinates of the optimized structures of PhMePz

atomic number	X-coordinate	Y-coordinate	Z-coordinate
6	7.391575278	1.622462748	0.248855138
6	7.645239674	0.433893003	0.925551662
6	6.726109963	-0.613809170	0.888386369
6	5.545583891	-0.504993260	0.140610304
6	5.303904196	0.699499678	-0.544983800
6	6.206873362	1.756364743	-0.473961518
7	4.611127541	-1.563627514	0.061723700
6	3.235328935	-1.270485882	0.084365613
6	2.740744961	-0.141546162	-0.597111580
16	3.863816201	0.823934851	-1.592404078
6	5.041801958	-2.895499307	0.476003506
6	2.310404644	-2.075919723	0.764251557
6	0.951481379	-1.781424932	0.742102960
6	0.460767138	-0.652051762	0.076965837
6	1.388563589	0.171838095	-0.578220862
6	-0.985248100	-0.327520236	0.068775935
6	-1.955747739	-1.333899663	0.026204216

6	-3.312092249	-0.991768119	0.006478785
7	-3.722210936	0.284597208	0.054768517
6	-2.807859511	1.264667748	0.110380217
6	-1.434866524	0.996490846	0.104234074
6	-3.327612198	2.659578384	0.161074173
6	-4.375965738	-2.032631198	-0.050718609
6	-4.589144084	2.954545354	-0.376430400
6	-5.089949119	4.252107162	-0.345859671
6	-4.344065642	5.280243120	0.230715990
6	-3.093206145	4.998185032	0.777195418
6	-2.588729895	3.700553828	0.741907588
6	-4.144078288	-3.292346720	-0.621997600
6	-5.152005856	-4.252539701	-0.661987710
6	-6.409731450	-3.972627098	-0.130353447
6	-6.653730687	-2.721252441	0.435659849
6	-5.648993380	-1.759630936	0.471093539
1	8.100246116	2.441008632	0.283968341
1	8.556100566	0.316861224	1.501139444
1	6.933192103	-1.516609020	1.446555001
1	5.987408105	2.677696434	-1.001059736

1	5.061170772	-3.028014635	1.565245146
1	4.368306919	-3.635877948	0.045812537
1	6.041185478	-3.081225821	0.084326434
1	2.648618038	-2.936258597	1.325239106
1	0.272245354	-2.424731193	1.288523894
1	1.049282580	1.046188893	-1.120975905
1	-1.656716396	-2.372878241	-0.000243776
1	-0.722829806	1.809831071	0.135633135
1	-5.165562504	2.153224412	-0.820279294
1	-6.063712289	4.462304599	-0.774082189
1	-4.735526788	6.290857390	0.256848979
1	-2.510685633	5.787440066	1.238879512
1	-1.624346174	3.497991963	1.192478234
1	-3.180638816	-3.521250425	-1.061835606
1	-4.955758584	-5.217277356	-1.116093493
1	-7.193546357	-4.720958972	-0.160320424
1	-7.629047326	-2.494633713	0.851800716
1	-5.834974682	-0.786334770	0.906334516

Cartesian coordinates of the optimized structures of TolMePz

atomic number	X-coordinate	Y-coordinate	Z-coordinate
6	7.820894770	1.458338720	0.231088479
6	8.057511667	0.274730915	0.922506242
6	7.124223978	-0.760747102	0.896828450
6	5.946151065	-0.645000967	0.146206884
6	5.721836957	0.554242841	-0.554461274
6	6.639044801	1.599494418	-0.495029554
7	4.997354684	-1.691456507	0.078836198
6	3.625503846	-1.378763734	0.096731758
6	3.147369278	-0.251783346	-0.599372214
16	4.284997819	0.685102141	-1.605558943
6	5.409064945	-3.023869966	0.510168419
6	2.688893496	-2.162106287	0.786194278
6	1.334290826	-1.848254965	0.759666882
6	0.859889243	-0.720560932	0.080007019
6	1.799780032	0.081198197	-0.585280018
6	-0.581518795	-0.374934340	0.067408368
6	-1.566151351	-1.367703802	0.036808509

6	-2.917947858	-1.006374888	0.012593927
7	-3.308539343	0.277019626	0.046010573
6	-2.380138400	1.245057471	0.090159932
6	-1.010951377	0.956005670	0.086825929
6	-2.879117995	2.646567238	0.125286979
6	-3.995865546	-2.031335322	-0.032515475
6	-4.142020752	2.956977146	-0.398602680
6	-4.620799414	4.261700092	-0.383981473
6	-3.866611686	5.306831869	0.163199799
6	-2.609491249	4.994537535	0.691523627
6	-2.122273872	3.691147257	0.673802497
6	-3.785408712	-3.306827756	-0.572513580
6	-4.810055418	-4.249117961	-0.602355742
6	-6.078900417	-3.957519596	-0.092699264
6	-6.289249961	-2.678714666	0.439411581
6	-5.272474422	-1.732694142	0.466552015
6	-4.404235990	6.715939812	0.208424732
6	-7.182098612	-4.986807266	-0.097745072
1	8.540618321	2.267526549	0.257215815
1	8.965990362	0.152368933	1.500754055

1	7.318203001	-1.659362981	1.466325259
1	6.432877080	2.517176622	-1.033740951
1	5.425530930	-3.143157482	1.601016279
1	4.725750841	-3.760099085	0.088409201
1	6.406202525	-3.228283384	0.122054474
1	3.014499120	-3.020126698	1.358141072
1	0.645588751	-2.474660749	1.313805099
1	1.473214401	0.953444145	-1.139076090
1	-1.282011077	-2.411118034	0.023129420
1	-0.286625246	1.758788904	0.108266132
1	-4.738616135	2.160978970	-0.825386490
1	-5.596753161	4.474367232	-0.808829444
1	-2.003057477	5.781353734	1.128538477
1	-1.151722431	3.489830118	1.111980648
1	-2.824305483	-3.565671177	-1.001165133
1	-4.620926136	-5.224672704	-1.038464667
1	-7.265556638	-2.421398535	0.838238041
1	-5.453244154	-0.747728167	0.877434274
1	-4.977986479	6.885715696	1.126267191
1	-3.597258259	7.451617052	0.187535199

1	-5.071605877	6.914284441	-0.633258291
1	-7.303532831	-5.434820742	0.894504780
1	-8.141818016	-4.539815191	-0.369307222
1	-6.969986749	-5.795026510	-0.800411218

Cartesian coordinates of the optimized structures of PhMeO

atomic number	**X-coordinate**	**Y-coordinate**	**Z-coordinate**
6	0.730892975	-1.315388260	-0.030113467
6	-0.657408840	-1.133349434	-0.027985057
7	-1.210300183	0.089803600	-0.003675414
6	-0.414962692	1.171588841	-0.003144076
6	0.980104974	1.061125439	-0.047241392
6	1.579070965	-0.203136699	-0.050035159
6	3.052715285	-0.358913026	-0.073115771
6	-1.088938424	2.496131460	0.008912263
6	-1.591432503	-2.289237448	-0.018013703
6	-1.219313918	-3.552355194	-0.510444110
6	-2.101802433	-4.619922255	-0.492497233
6	-3.394782978	-4.460957261	0.024659440
6	-3.786316695	-3.210452439	0.514807934
6	-2.889338498	-2.145722467	0.484458279

6	3.889316136	0.540416646	0.597618426
6	5.275747526	0.401817417	0.586687952
6	5.860844994	-0.657116565	-0.114892268
6	5.038317199	-1.566251381	-0.794983849
6	3.661854413	-1.418189053	-0.769709915
6	-2.406980296	2.622991651	-0.443483851
6	-3.064347903	3.850479749	-0.453674019
6	-2.403681088	4.994784380	0.005881857
6	-1.086507394	4.884425671	0.472246893
6	-0.444551844	3.656943071	0.471260171
8	7.198174223	-0.887788457	-0.196295783
6	8.087974231	0.010875669	0.467302663
8	-2.946344578	6.241801918	0.043155161
6	-4.288784511	6.415506149	-0.411078123
8	-4.184726457	-5.568330469	0.003036861
6	-5.515490110	-5.467710008	0.510585883
1	1.148420482	-2.311738800	0.021792551
1	1.594085496	1.948648752	-0.117978912
1	-0.234635263	-3.702939306	-0.936645810
1	-1.814721759	-5.588946897	-0.882991492

1	-4.776461955	-3.056070983	0.921801034
1	-3.194587319	-1.179158076	0.863742675
1	3.456162475	1.356042895	1.164935860
1	5.881605940	1.113889941	1.130134021
1	5.503296014	-2.376488309	-1.343737529
1	3.049433804	-2.122395053	-1.320722631
1	-2.920741252	1.739258469	-0.799086841
1	-4.079973412	3.903304624	-0.821756138
1	-0.589616123	5.774641279	0.839021535
1	0.565681891	3.602285163	0.858919446
1	7.914202424	0.016542062	1.547589543
1	9.089706764	-0.362098389	0.264216197
1	7.991411766	1.027491256	0.074243831
1	-4.990289993	5.826637865	0.187658304
1	-4.507796919	7.474172227	-0.287424868
1	-4.389763416	6.144254654	-1.466404752
1	-5.517236236	-5.194302586	1.570128240
1	-6.103757989	-4.740193221	-0.056965225
1	-5.952340534	-6.457234739	0.392030355

Cartesian coordinates of the optimized structures of TolPz

atomic number	X-coordinate	Y-coordinate	Z-coordinate
6	8.075508826	0.106347308	-1.616068720
6	8.299384617	-0.993289753	-0.790570257
6	7.339953403	-1.379467164	0.141482298
6	6.155699012	-0.648845233	0.286357249
6	5.942246266	0.468660063	-0.535984855
6	6.887938399	0.826659918	-1.494102815
7	5.196792339	-1.025338674	1.239321237
6	3.826193821	-0.841798372	1.038989728
6	3.351174217	0.253720650	0.298954941
16	4.503249959	1.497549215	-0.269300674
6	2.894553540	-1.737769867	1.575439920
6	1.532170779	-1.544911266	1.386822648
6	1.049897685	-0.466944305	0.631967808
6	1.988670883	0.420261325	0.083029254
6	-0.402610437	-0.266834093	0.413444017
6	-1.271752828	-1.353142220	0.266895538
6	-2.634841093	-1.129122631	0.043596302
7	-3.150207340	0.108987753	-0.009778097

6	-2.336448415	1.165070329	0.143190818
6	-0.959534235	1.014313425	0.342317477
6	-3.589461737	-2.257934698	-0.128401136
6	-2.967935528	2.510582486	0.070680557
6	-4.164346740	2.688593759	-0.638586413
6	-4.762448971	3.939672453	-0.728723158
6	-4.199504964	5.060895679	-0.106489268
6	-3.010092418	4.880395632	0.606918213
6	-2.403269166	3.630946651	0.695309769
6	-3.179349121	-3.511221405	-0.603609612
6	-4.090776883	-4.551976176	-0.755040762
6	-5.442474127	-4.385541793	-0.435655338
6	-5.851381188	-3.130239715	0.030951006
6	-4.946745018	-2.085575604	0.178792368
6	-4.869883071	6.410692435	-0.180153021
6	-6.422669357	-5.524794157	-0.569428762
1	8.813654625	0.402791642	-2.351294414
1	9.216325332	-1.564222817	-0.877958540
1	7.505596306	-2.249565755	0.767976299
1	6.699441282	1.681587738	-2.133255972

1	5.435511848	-1.853436568	1.766908256
1	3.245625978	-2.585048732	2.154777737
1	0.837858028	-2.238950332	1.844569896
1	1.655258592	1.251365338	-0.526890810
1	-0.888893258	-2.363252348	0.316818409
1	-0.328431938	1.886016090	0.448578729
1	-4.612323306	1.832032401	-1.125706548
1	-5.681152963	4.050035956	-1.296241188
1	-2.552713409	5.728719330	1.105862968
1	-1.493188873	3.531317609	1.275244006
1	-2.146510692	-3.675501047	-0.887716611
1	-3.746265815	-5.507133554	-1.138158655
1	-6.895058002	-2.968801035	0.281799874
1	-5.281229718	-1.120340538	0.536829665
1	-5.625873150	6.515071801	0.605986665
1	-4.149655033	7.221316996	-0.050952267
1	-5.376712053	6.551020875	-1.137733752
1	-6.510070864	-6.077804808	0.372402877
1	-7.420691775	-5.163206814	-0.827373926
1	-6.105791882	-6.234764443	-1.336418663

Cartesian coordinates of the optimized structures of PhPz.

atomic number	X-coordinate	Y-coordinate	Z-coordinate
6	-7.674299178	0.240232860	1.570746832
6	-7.901480580	-0.869206742	0.759375739
6	-6.937894954	-1.277724530	-0.158773154
6	-5.745758362	-0.560140717	-0.303918111
6	-5.528643921	0.566928066	0.504156268
6	-6.479009060	0.947638515	1.448766528
7	-4.782277333	-0.959400300	-1.243044385
6	-3.411990727	-0.786139022	-1.033736950
6	-2.932680311	0.314798217	-0.304307269
16	-4.077257638	1.577811645	0.235815102
6	-2.484555670	-1.698113430	-1.550319299
6	-1.122191018	-1.516591764	-1.351445191
6	-0.636148699	-0.433687663	-0.606134205
6	-1.570634234	0.470627467	-0.078111396
6	0.815921842	-0.246375326	-0.375703749
6	1.672165266	-1.339807642	-0.206410919
6	3.034692021	-1.127131808	0.028083326
7	3.563718121	0.105132467	0.070617939

6	2.762778520	1.167048309	-0.104079381
6	1.386689528	1.029350954	-0.314958173
6	3.975999015	-2.264579143	0.225902996
6	3.408728910	2.507727590	-0.042516269
6	4.590978069	2.679888349	0.692157010
6	5.204871277	3.925812676	0.771107631
6	4.654545020	5.023686628	0.109549030
6	3.485703478	4.863280754	-0.632704613
6	2.867527378	3.617568040	-0.707571700
6	3.543295785	-3.499090889	0.731732959
6	4.439206928	-4.551168758	0.904884470
6	5.783737942	-4.389968032	0.574551499
6	6.226905737	-3.164871276	0.075993444
6	5.333539762	-2.111713706	-0.092313497
1	-8.415883994	0.554171211	2.295169658
1	-8.824416291	-1.430316573	0.847186073
1	-7.106179299	-2.155408628	-0.773904777
1	-6.287911301	1.809930175	2.077167692
1	-5.024888940	-1.792059923	-1.761567074
1	-2.838810120	-2.549091074	-2.122174878

1	-0.430864788	-2.223482746	-1.793745982
1	-1.234377616	1.306552752	0.523637852
1	1.279416119	-2.346506106	-0.247486306
1	0.766592156	1.906719547	-0.438116735
1	5.015045275	1.824439766	1.201808899
1	6.113492575	4.041158134	1.351494204
1	5.134069976	5.994146278	0.168948834
1	3.056942930	5.707175308	-1.161336296
1	1.972429978	3.508722519	-1.308448233
1	2.507303783	-3.637216708	1.017579084
1	4.086950789	-5.494863945	1.305911129
1	6.480363012	-5.209831584	0.708025237
1	7.270950542	-3.030345063	-0.184045413
1	5.673813645	-1.158672709	-0.476182623

8. Cyclic voltammetry graphs

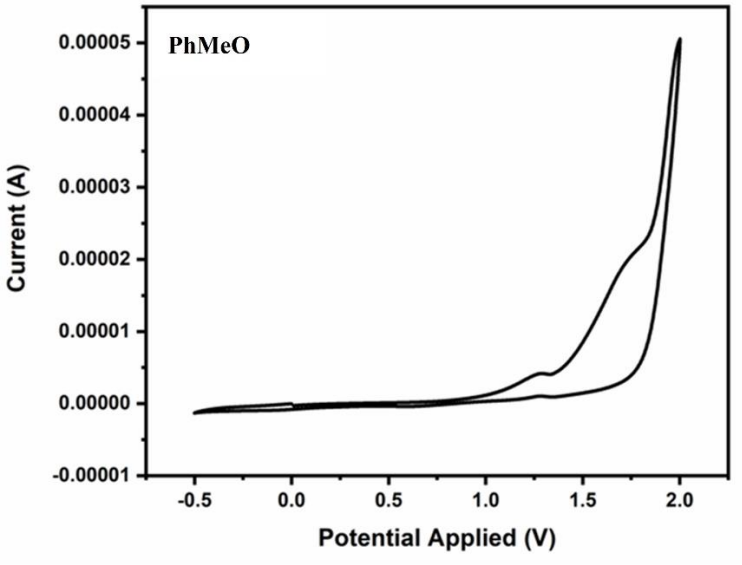

Fig. S16. Cyclic Voltammetry graph of **PhMeO** (Ag/AgCl (reference electrode), 0.1M tetrabutylammonium hexafluorophosphate (supporting electrolyte)).

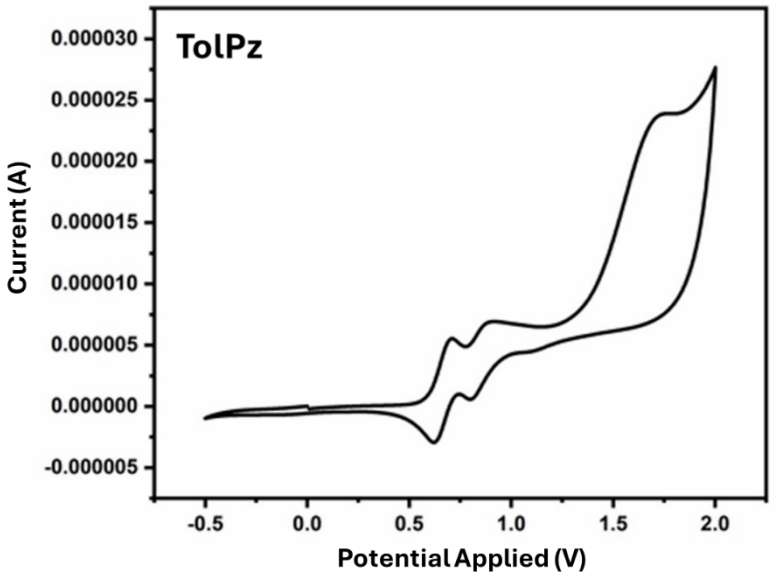

Fig. S17. CV graph of **TolPz** (Ag/AgCl (reference electrode), 0.1M tetrabutylammonium hexafluorophosphate (supporting electrolyte)).

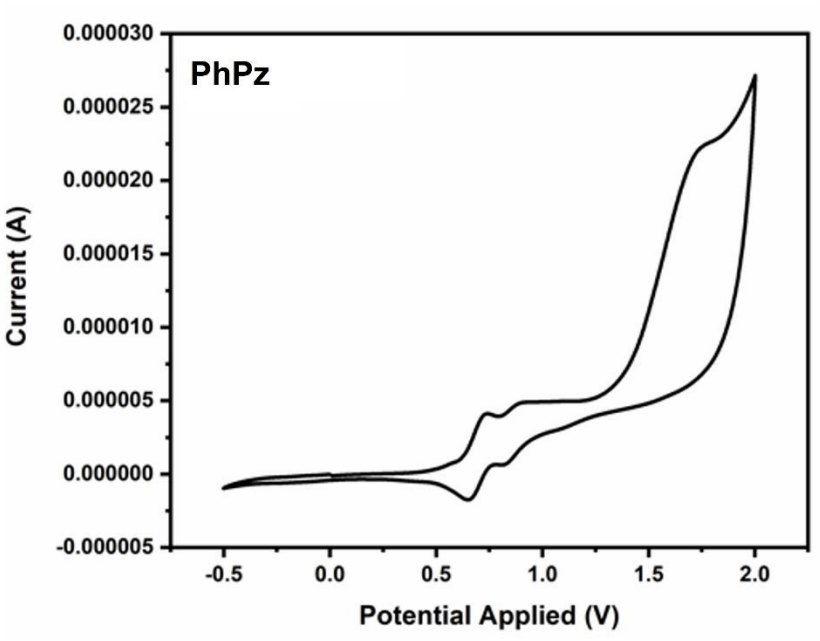

Fig. S18. CV graph of **PhPz** (Ag/AgCl (reference electrode), 0.1M tetrabutylammonium hexafluorophosphate (supporting electrolyte)).

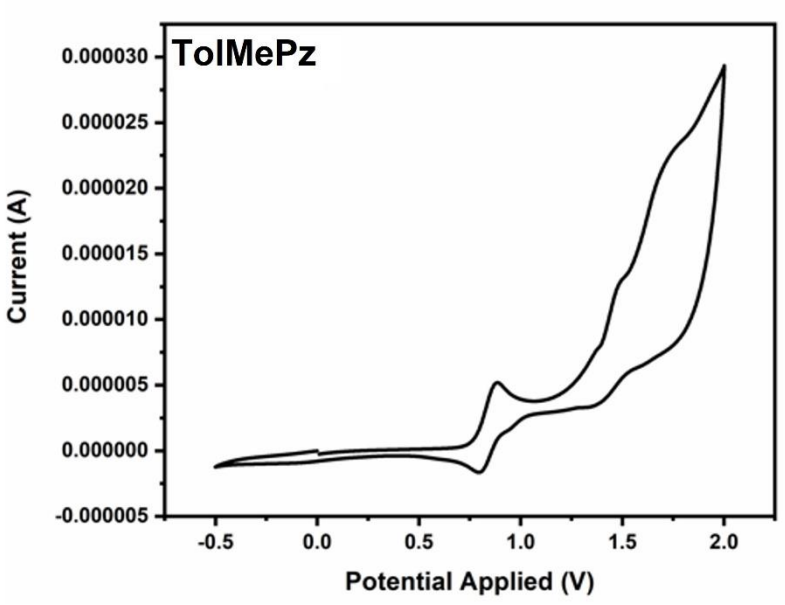

Fig. S19. CV graph of **TolMePz** (Ag/AgCl (reference electrode), 0.1M tetrabutylammonium hexafluorophosphate(supporting electrolyte)).

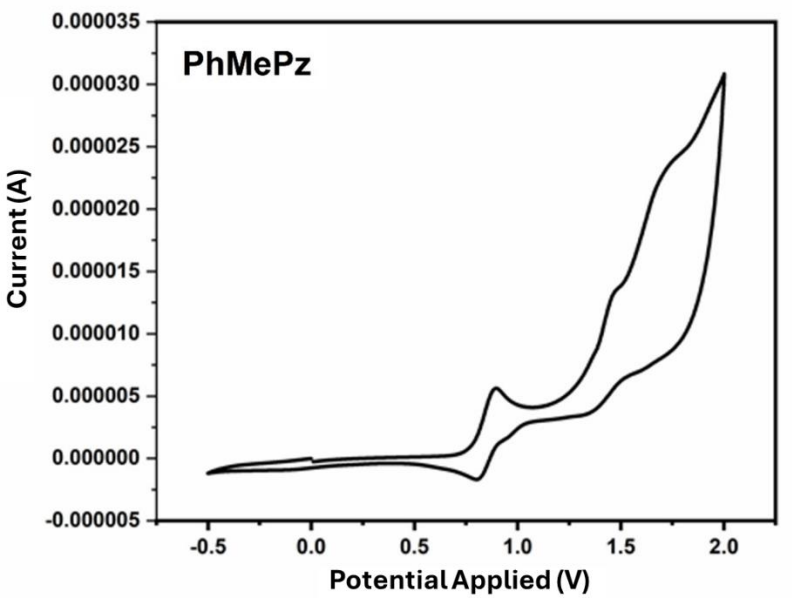

Fig. S20. CV graph of **PhMePz** (Ag/AgCl (reference electrode), 0.1M tetrabutylammonium hexafluorophosphate (supporting electrolyte)).

9.TGA/DSC graphs

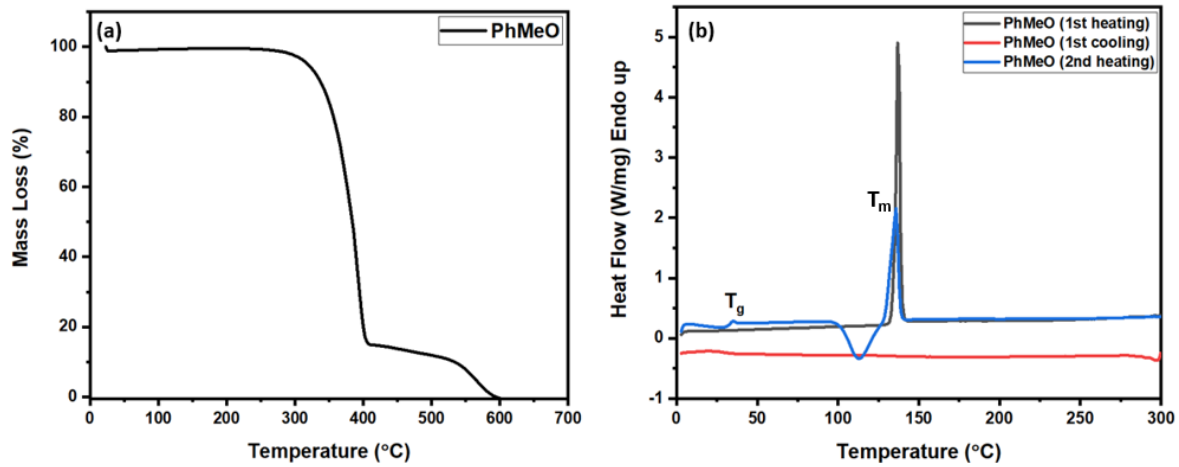

Fig. S21. TGA/DSC graph of **PhMeO**

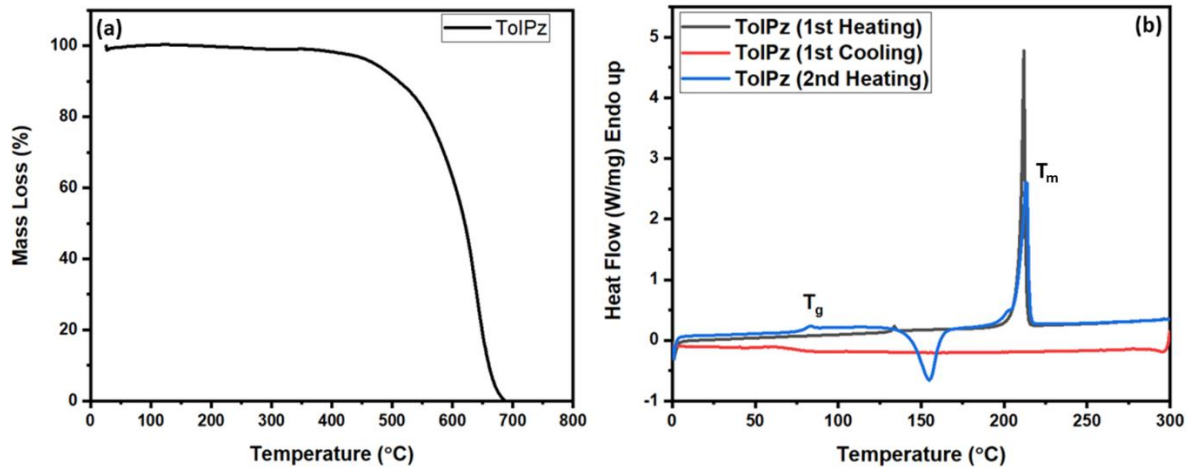

Fig. S22. TGA/DSC graph of **TolPz**

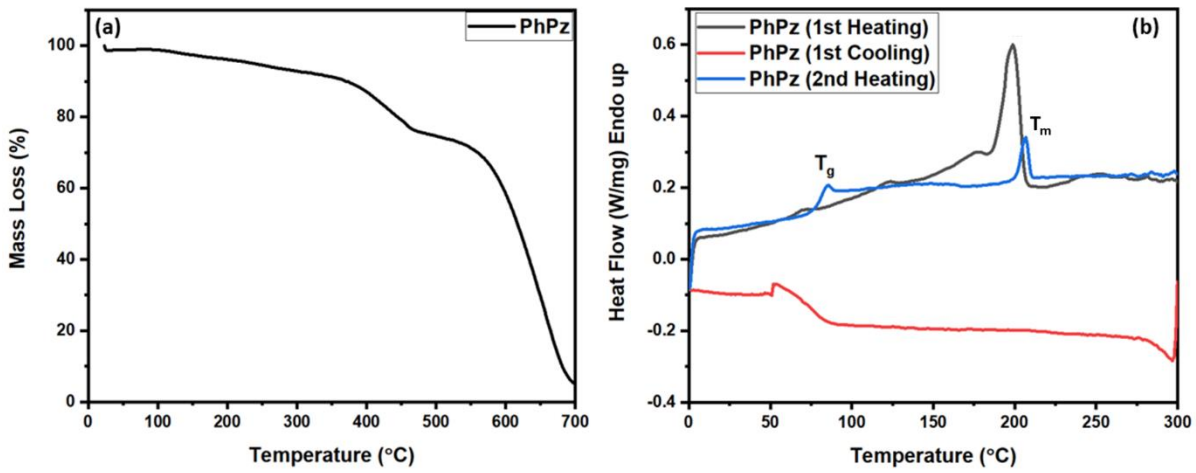

Fig. S23. TGA/DSC graph of **PhPz**

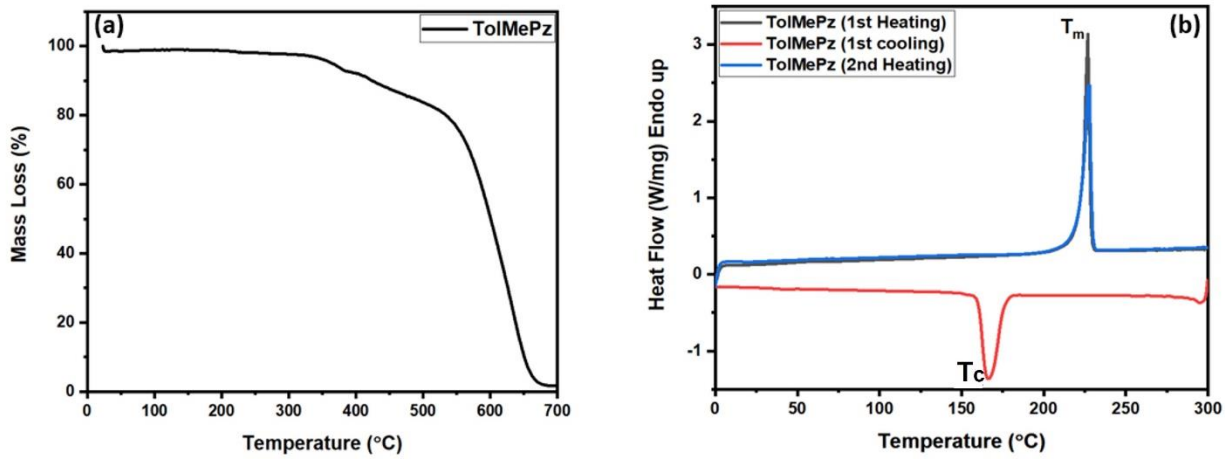

Fig. S24. TGA/DSC graph of **TolMePz**

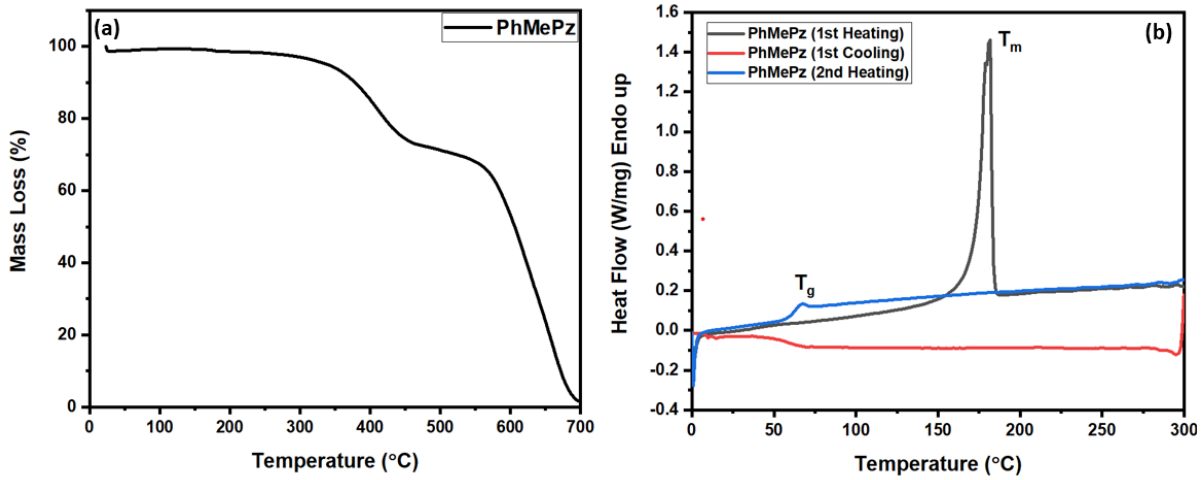

Fig. S25. TGA/DSC graph of **PhMePz**

10. Single crystal analysis

Single-crystal X-ray diffraction data of compounds **PhPz**, **TolPz**, and **PhMePz** were collected on an Agilent Supernova X-ray diffractometer equipped with a CCD detector at room temperature (150 or 296 K) using the source graphite-monochromatic Cu Kα radiation (λ = 1.54184Å). For single crystal analysis, the same methods and software were used as mentioned in the previous report.[6-10] Compounds **PhPz** and **TolPz** contain disordered DMSO molecules which we have modelled reliably using PART instruction. In **PhPz** the S-atom of the DMSO was disordered with 0.91 in PART 1 and 0.09 in PART 2 whereas in **TolPz** the S and O-atoms of DMSO was disordered with 0.63 in PART 1 and 0.37 in PART 2. Compound **TolPz** contains a disordered DMSO molecules which could be modelled reliably. Crystallographic data is summarized in **Table S10**. These data can be obtained free of charge from The Cambridge Crystallographic Data Centre *via* www.ccdc.cam.ac.uk/data_request/cif.

Table S10. **Crystal data and structure refinement for PhPz**, **TolPz**, and **PhMePz**

Identification code	**PhPz**	**TolPz**	**PhMePz**
Empirical formula	$C_{31}H_{26}N_2OS_2$	$C_{33}H_{30}N_2OS_2$	$C_{30}H_{22}N_2S$
Formula weight	506.66	534.75	442.58
Temperature/K	293(2)	293(2)	293(2)
Crystal system	Monoclinic	Monoclinic	triclinic
Space group	$P2_1/c$	$P2_1/n$	P-1
a/Å	16.2678(6)	5.8344(2)	7.5356(8)
b/Å	21.7983(8)	18.1183(6)	9.0697(7)
c/Å	7.4971(3)	26.5642(7)	16.4415(12)
α/°	90.00	90.00	85.207(6)
β/°	100.634(4)	94.910(2)	84.755(7)
γ/°	90.00	90.00	84.765(7)
Volume/$Å^3$	2612.89(17)	2797.78(15)	1111.12(17)
Z	4	4	2

ρ_{calc}g/cm^3	1.288	1.270	1.323
μ/mm^{-1}	2.051	1.941	1.445
F(000)	1069	1133	465
Radiation	CuKα (λ = 1.54184)	CuKα (λ = 1.54184)	CuKα (λ = 1.54184)
Index ranges	-19 ≤ h ≤ 18 0 ≤ k ≤ 25 0 ≤ l ≤ 8	-6 ≤ h ≤ 4 -21 ≤ k ≤ 19 -28 ≤ l ≤ 31	-8 ≤ h ≤ 8 -10 ≤ k ≤ 9 -19 ≤ l ≤ 19
Reflections collected	8632	8917	6325
Data/restraints/parameters	4596/49/356	4888/60/390	3877/42/300
Goodness-of-fit on F^2	1.047	1.056	1.003
Final R indexes [I>=2σ (I)]	R_1 = 0.0486, wR_2 = 0.1296	R_1 = 0.0455, wR_2 = 0.1211	R_1 = 0.0430, wR_2 = 0.1028
Final R indexes [all data]	R_1 = 0.0613, wR_2 = 0.1435	R_1 = 0.0591, wR_2 = 0.1322	R_1 = 0.0710, wR_2 = 0.1314
CCDC No.	2248255	2248257	2248258

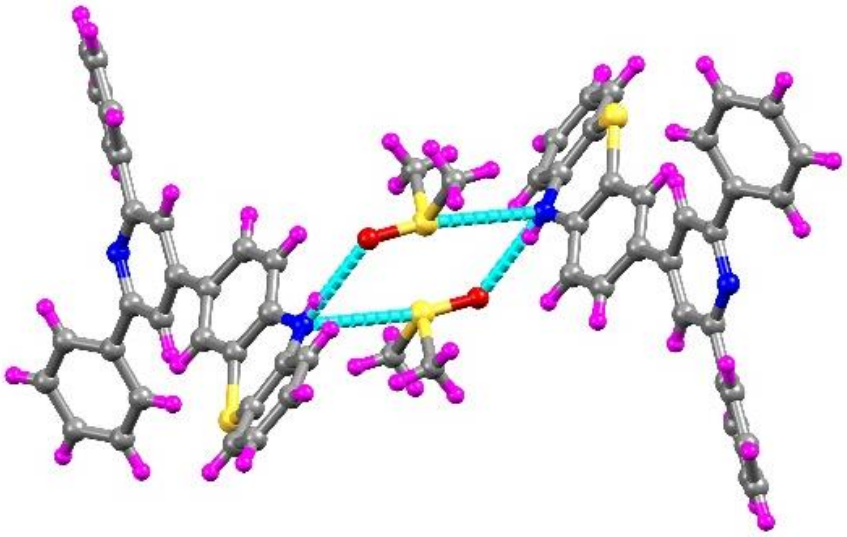

A

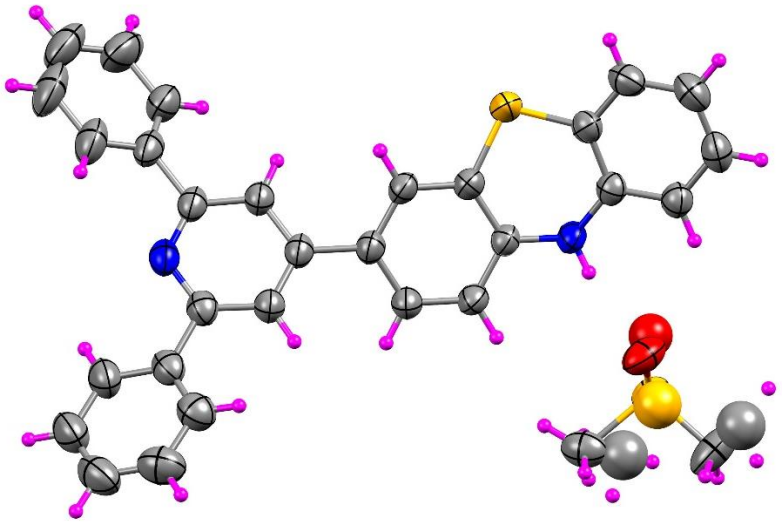

B

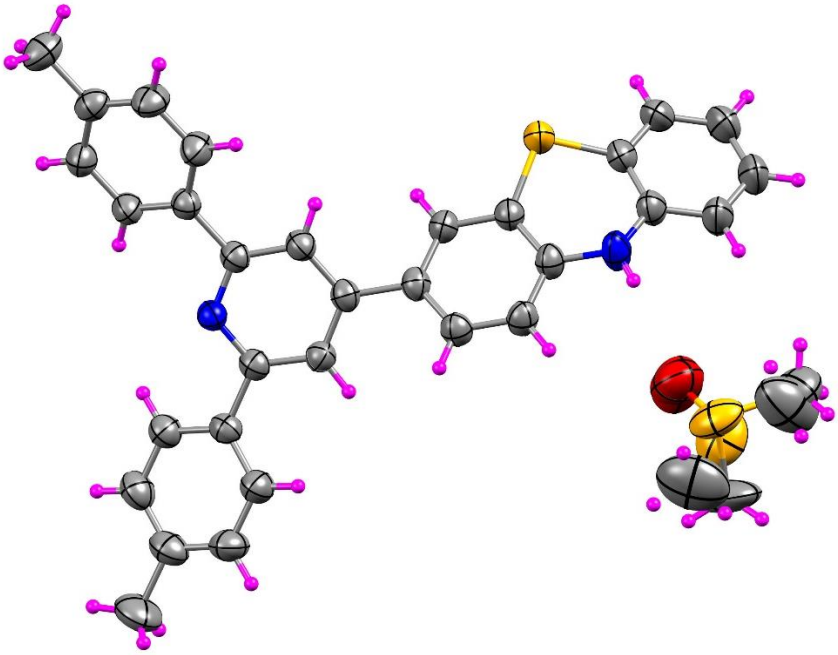

C

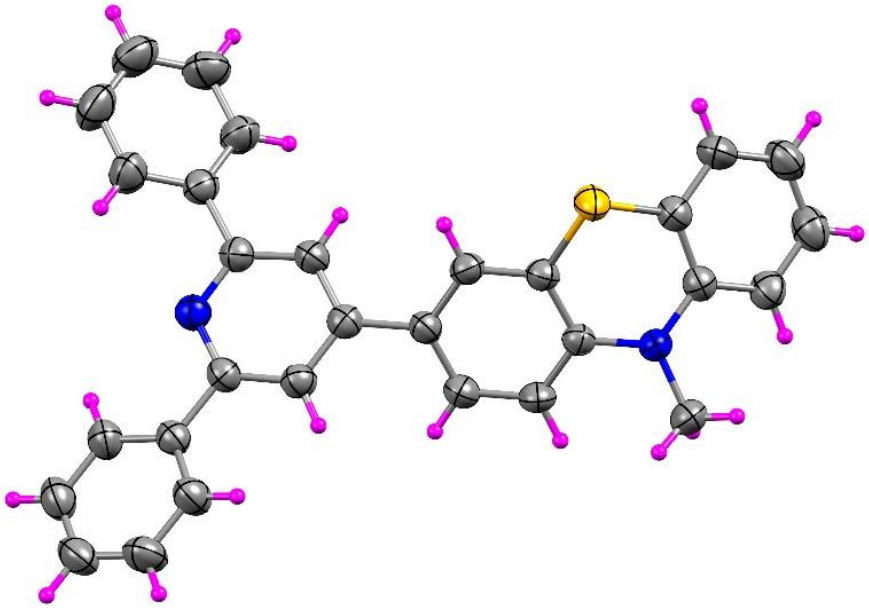

D

Fig. S26: (A) Cyclic hydrogen-bonded network between **PhPz** and DMSO molecules. ORTEP drawings of **PhPz** (B), **TolPz** (C) and **PhMePZ** (D) with ellipsoid contour probability level of 50%.

11.Hole-only device fabrication

The HODs were consisted of ~125 nm indium tin oxide (ITO) as anode layer, ~40 nm poly(3,4-ethylenedioxythiophene): polystyrene sulphonate (PEDOT:PSS) as hole injection layer (HIL), ~10 nm hole transport layer (HTL), ~1 nm lithium fluoride (LiF) as electron injection layer (EIL), and ~100 nm aluminum (Al) as cathode layer.

Before fabricating the device, the ITO-coated glass substrate was first cleaned in acetone at 45°C for 30 mins and then in 2-propanol at 60°C for 60 mins (both under an ultrasonic bath), followed by treating them in an ozone atmosphere under ultraviolet light for 15 min. After cleaning, the substrate was transferred into a nitrogen-filled glove box to coat the HIL and HTL via spin-coating. The HIL was spin-coated at 4,000 rpm for 20 seconds, then heated at 120 °C for 10 min, and then cooled down for 10 minutes. After dissolving the compounds in toluene, they were spin-coated onto the specimen at 2,500 rpm for 20 seconds for coating the HTL and then heated at 120 °C for 10 min, and then cooled down for 10 minutes. After coating the HTL, the coated substrate was transferred into a high-vacuum chamber with a base pressure of ~1×10^{-7} torr. The EIL and cathode were sequentially deposited via thermal evaporation. The current density of the fabricated device was measured using a Keithley 2400 electrometer.

12.References

(1) F. Liu, J. Du, D. Song, M. Xu, G. Suna, Sensitive Fluorescent Sensor for the Detection of Endogenous Hydroxyl Radicals in Living Cells and Bacteria and Direct Imaging with Respect to Its Ecotoxicity in Living Zebra Fish. *Chem. Commun*. 2016, **52**, 4636–4639.

(2) J. Liaw, K.-L. Wang, S.-P. Pujari, Y.-C. Huang, B.-C. Tao, M.-H. Chen, K.-R. Lee, J.-Y. Lai. A Novel, Conjugated Polymer Containing Fluorene, Pyridine and Unsymmetric Carbazole Moieties: Synthesis, Protonation and Electrochemical Properties. *Dye. Pigment.* 2009, **82**, 109–117.

(3) M. Li, T. Wang, C. Wang. Multicomponent Reaction of Pyridinium Salts, β-Nitrostyrenes and Ammonium Acetate under the DBU/Acetic Acid System: Access to 2,4,6-Triarylpyridine Derivatives. *Chem. Select.* 2020, **5**, 3600–3604.

(4) J.-V. Allan, G. Reynolds. Synthesis of some phenothiazinyl and carbazolyl pyrylium salts. *J. Hetro. Chem.* 1976, **13**, 73-76.

(5) M. J. Frisch, G. W. Trucks, H. B. Schlegel, G. E. Scuseria, M. A. Robb, J. R. Cheeseman, G. Scalmani, V. Barone, B. Mennucci, G. A. Petersson, H. Nakatsuji, M. Caricato, X. Li, H. P. Hratchian, A. F. Izmaylov, J. Bloino, G. Zheng, J. L. Sonnenberg, M. Hada, M. Ehara, K. Toyota, R. Fukuda, J. Hasegawa, M. Ishida, T. Nakajima, Y. Honda, O. Kitao, H. Nakai, T. Vreven, J. A. Montgomery, J. E. Peralta, F. Ogliaro, M. Bearpark, J. J. Heyd, E. Brothers, K. N. Kudin, V. N. Staroverov, R. Kobayashi, J. Normand, K. Raghavachari, A. Rendell, J. C. Burant, S. S. Iyengar, J. Tomasi, M. Cossi, N. Rega, J. M. Millam, M. Klene, J. E. Knox, J. B. Cross, V. Bakken, C. Adamo, J. Jaramillo, R. Gomperts, R. E. Stratmann, O. Yazyev, A. J. Austin, R. Cammi, C. Pomelli, J. W. Ochterski, R. L. Martin, K. Morokuma, V. G. Zakrzewski, G. A. Voth, P. Salvador, J. J. Dannenberg, S.

Dapprich, A. D. Daniels, O¨. Farkas, J. B. Foresman, J. V. Ortiz, J. Cioslowski and D. J. Fox, Gaussian, Inc., Wallingford CT, 2016.

(6) A. Karmakar, M. M.-A. Soliman, G. M.-D. M. Rúbio, M. F.C. G. da Silva, A. J. L. Pombeiro. Synthesis and catalytic activities of a Zn(II) based metallomacrocycle and a metal–organic framework towards one-pot deacetalization-Knoevenagel tandem reactions under different strategies: a comparative study. *Dalton Trans.*, 2020, **49**, 8075–8085.

(7) Crys AlisPro Program, ver. 171.37.33c. Data Collection and Processing Software for Agilent X-ray Diffractometers; Agilent Technologies: Oxford, UK, **2012**, 1−49

(8) G. M. Sheldrick. SADABS. Program for Empirical Absorption Correction. University of Gottingen, Germany, **1996**.

(9) G. M. Sheldrick. Crystal structure refinement with *SHELXL*. *Acta Crystallogr*. 2015, **C71**, 3–8.

(10) L. J. Farrugia. WinGX and ORTEP for Windows: an update. *J. Appl. Crystallogr*. 2012, **45**, 849–854.